




A framework employing the AHP and FR methods to assess the landslide susceptibility of the Western Ghats region in Kollam district

B. G. Babitha¹ · Jean Homian Danumah² · G. S. Pradeep³ · Romulus Costache⁴ · Nilanchal Patel⁵ · Megha K. Prasad⁶ · A. Rajaneesh⁷ · Pratheesh C. Mammen³ · R. S. Ajin^{3,8}  · Sekhar L. Kuriakose³

Received: 1 March 2022 / Revised: 3 June 2022 / Accepted: 14 June 2022 / Published online: 28 June 2022
© The Author(s), under exclusive licence to Springer Nature Switzerland AG 2022

Abstract

Landslides are the most frequently occurring geohazard in the Western Ghats due to the steep terrain and heavy rainfall the area receives. This research aims to develop a framework to demarcate the zones susceptible to landslides employing geographic information system (GIS) technique. The Western Ghats region in Kollam district is selected for the modelling. Landsat satellite images, digital elevation model, published topographic, soil and geological maps, Google Earth Pro are the sources used in the study. Ten major parameters that impact landslide susceptibility are used, which include slope angle, elevation, slope aspect, stream buffer, lithology, soil, road buffer, normalized difference vegetation index, land use and land cover, and lineament buffer. Analytical hierarchy process (AHP) and frequency ratio (FR) methods were used to determine the relative weights of each parameter on landslide susceptibility, and the maps were prepared using ArcGIS software. The study area was demarcated into five zones of susceptibility. According to the analysis, 33% and 23% of the area are classified as high and very high susceptible zones in maps generated using the AHP and FR methods, respectively. The landslide occurrence in this area can be attributed to both natural as well as anthropogenic activities (mainly due to road cuttings). To validate the result of this study, the landslide incidence data collected from the National Remote Sensing Centre has been utilized. The validation confirmed that the results are outstanding, with an AUC value of 0.906 and 0.926 for the AHP and FR methods, respectively. The outcome of the study is useful for land-use planners, policymakers, and the government in taking effective preventive and mitigation measures in the areas of higher susceptibility to minimize the loss of property and fatalities.

Keywords Analytical hierarchy process · Anthropogenic factors · Frequency ratio · Slope failures · Western ghats

✉ R. S. Ajin
ajinares@gmail.com; ajinares@ieee.org

¹ Department of Civil Engineering, College of Engineering, Pathanapuram, Kollam, Kerala, India

² Centre Universitaire de Recherche et d'Application en Télédétection (CURAT), Université Félix Houphouët-Boigny, Abidjan, Ivory Coast

³ Kerala State Emergency Operations Centre, Kerala State Disaster Management Authority, Thiruvananthapuram, India

⁴ National Institute of Hydrology and Water Management, Bucharest, Romania

⁵ Department of Remote Sensing, Birla Institute of Technology Mesra, Ranchi, Jharkhand, India

⁶ Department of Remote Sensing, Bharathidasan University, Tiruchirappalli, Tamil Nadu, India

⁷ Department of Geology, University of Kerala, Thiruvananthapuram, India

⁸ Resilience Development Initiative (RDI), Bandung, Indonesia

Introduction

Landslides, the most common geohazard occurring in mountainous terrain, can cause serious damage to natural resources and infrastructures, as well as loss of life and property (Pourghasemi et al. 2012a). The landslide hazard of an area is determined by the combined effects of intrinsic as well as extrinsic variables (Dahal and Dahal 2017). The intrinsic variables that influence the susceptibility to landslides include the geology of the bedrock, the geomorphology, the soil type and depth, the slope aspect and angle, the convexity and concavity of the slope, the elevation, the land-use pattern, the drainage pattern, and the engineering properties of the slope material (Dahal et al. 2008). The extrinsic variables that trigger landslides are heavy rainfall, earthquakes, volcanoes (Dahal et al. 2008), and human activities (Trianawati and Rahmafritria 2016). Human activities such as excavation work and tunnelling can change the natural equilibrium of slopes and lead to slope failures (Achour and Pourghasemi 2020). The duration of rainfall triggers landslides in a different manner.

Slow-moving deep-seated landslides (e.g., earthflows, slumps) are activated by prolonged rainfall which lasts for several days or weeks, whereas fast-moving shallow landslides (e.g., debris flow) are triggered by individual high-intensity rainfall events (Sidle 2007).

The most landslide-vulnerable areas in India include the Meghalayan plateau, the Western Ghats, and the Himalayan Mountain regions, which together constitute about 15% of the total land area (NDMA 2009). This is a matter of concern because of the rapid population expansion in the mountainous region (van Westen et al. 2012). A large number of landslides occurred in the Western Ghats region in Kerala during the 2018 and 2019 monsoons and caused substantial loss of life and property damage. The damage to roads, buildings, and livestock was particularly high. One of the best strategies to reduce landslide-related damage and loss is the preparation of a landslide susceptible zone map. Susceptible zone maps are important in mitigating landslide risks as they show the zones of potential slope failures. The land use data should be updated every 1–10 years, which depends on the dynamics of land use change in the area (van Westen et al. 2008). Land use data

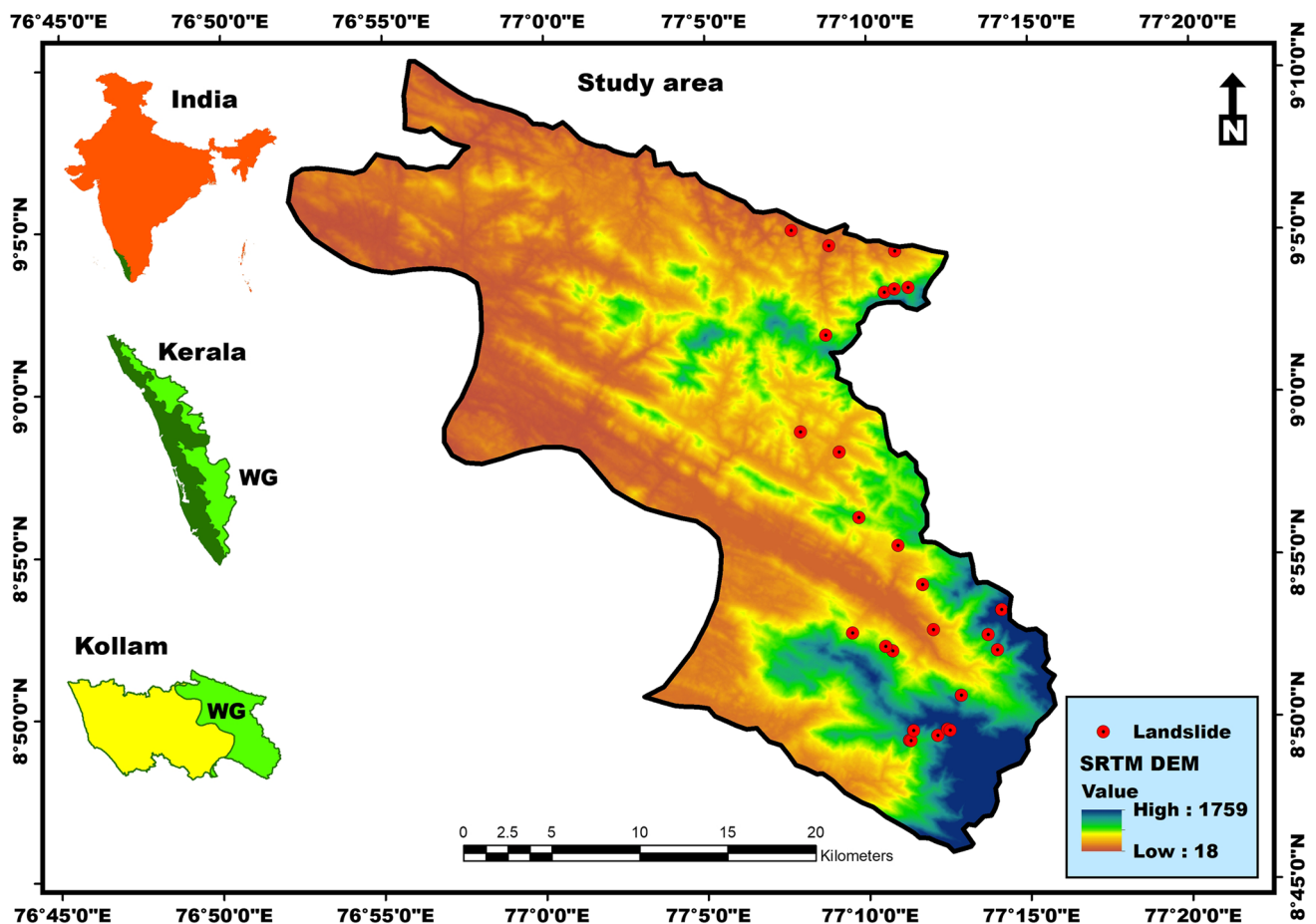
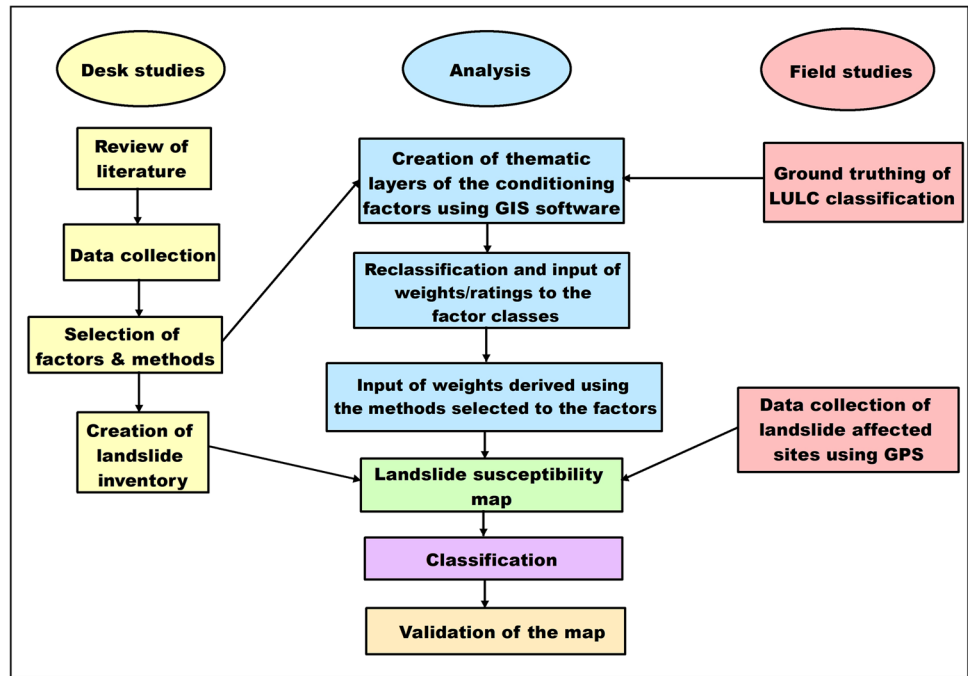


Fig. 1 Location of the study area

Fig. 2 Framework for the landslide susceptibility modelling



is an important factor used in susceptible zone mapping and, therefore, the map too needs to be updated whenever changes in land use occur.

The methods used to create the susceptibility maps can be either quantitative or qualitative (Guzzetti et al.

1999). Qualitative (subjective) methods depend on expert knowledge (Aleotti and Chowdhury 1999) and quantitative (objective) methods use numerical tools to assess the correlation between landslides and the causative/conditioning factors (Guzzetti et al. 1999). Quantitative methods

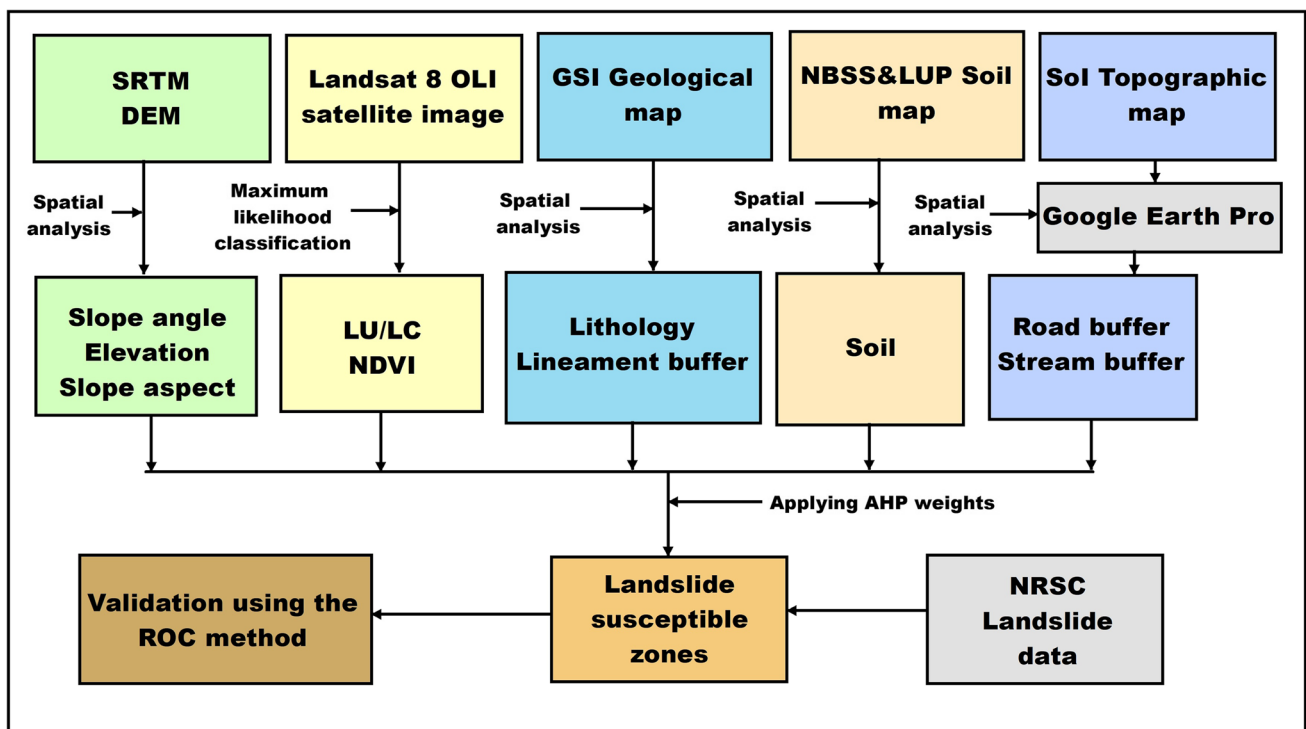


Fig. 3 Flowchart – landslide susceptibility modelling

Table 1 Data source	Data	Source	Thematic layers derived	Scale/spatial resolution
	Topographic map	Survey of India	Road buffer Stream buffer	1:50000
	Geological map	Geological Survey of India	Lithology	1:250,000
	Soil map	National Bureau of Soil Survey & Land Use Planning	Soil texture	1:250,000
	SRTM DEM	https://earthexplorer.usgs.gov/	Slope, Elevation, Aspect,	30 m
	Landsat 8 OLI image	https://earthexplorer.usgs.gov/	Land use/land cover NDVI	30 m
	Lineament data	http://www.bhuvan.nrsc.gov.in/	Lineament density	1:50,000
	Google Earth Pro	https://earth.google.com/web/	Road buffer (updated)	15 cm–15 m

include weights of evidence (Pradhan et al. 2010a; Prasanakumar and Vijith 2012; Polykretis and Chalkias 2018; Quinn et al. 2010), logistic regression (Hemasinghe et al.

2018; Lombardo and Mai 2018; Oh et al. 2018), artificial neural networks (Lee 2007, Ortiz and Martínez-Graña 2018, Pascale et al. 2013, Shahri et al. 2019), and AHP

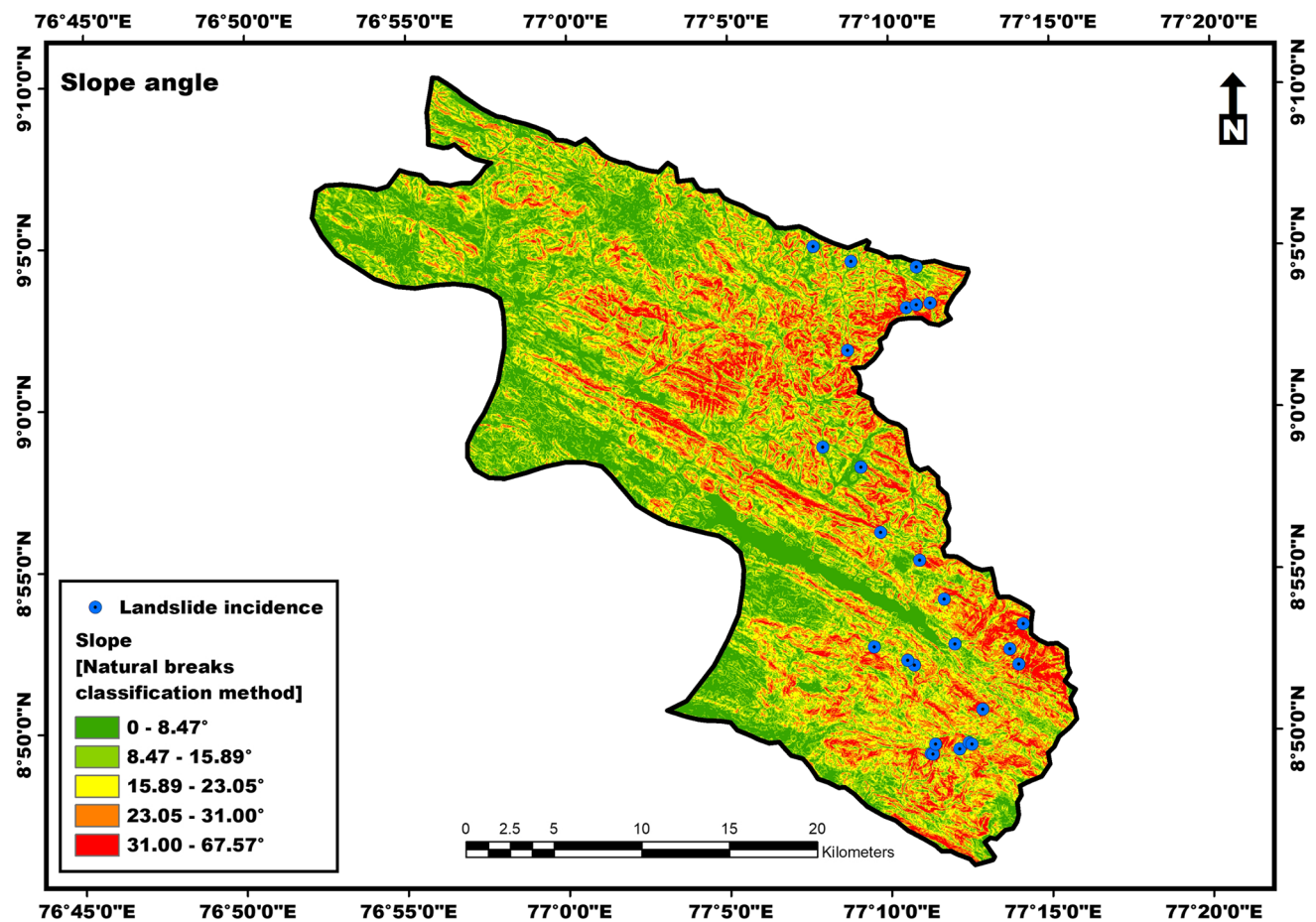


Fig. 4 Slope angle

(Achour et al. 2017; El Jazouli et al. 2019; Nguyen and Liu 2019; Yalcin 2008). Researchers have also used methods such as fuzzy logic (Fatemi Aghda et al. 2018; Sharma et al. 2013), Shannon’s entropy (Sharma et al. 2012, 2015), random forest (Catani et al. 2013; Lai et al. 2018; Taalab et al. 2018; Youssef et al. 2016), decision tree (Nefeslioglu et al. 2010; Zhang et al. 2017), support vector machine (Ballabio and Sterlacchini 2012; Lee et al. 2017; Pourghasemi et al. 2013), and Naive Bayes classifier (Bui et al. 2012; Lee et al. 2019) to produce landslide vulnerability/susceptibility maps.

The AHP (Saaty 1980) is a semi-quantitative analytical method for decision making where decisions are made using weights by relative comparison in pairs. This method has been used by many researchers to delineate landslide susceptible zones. El Jazouli et al. (2019) prepared the landslide susceptibility map of the Oum Er-Rbia high basin in Morocco using the AHP method. They used eight conditioning factors such as slope gradient, elevation, slope aspect, land cover, lithology, distance to road, distance to fault, and distance to drainage network. Semlali et al. (2019) created the landslide susceptible zone map of the Oued Laou

watershed in Morocco using the same method using the factors slope, aspect, land cover, drainage density, lithology, distance from river, distance from fault, and distance from road. FR is a bivariate statistical method widely employed in demarcating susceptible zones (Jana et al. 2019; Oh et al. 2017; Sharma et al. 2014; Silalahi et al. 2019; Yilmaz 2009).

No other researchers attempted to demarcate landslide susceptibility zones of this data-scarce region in the Western Ghats, which employed two different models (AHP and FR). There are no validated susceptibility maps available for the Western Ghats region, which are created using multi-criteria decision-making methods. Abrams et al. (2018) pointed out that the models like AHP and FR are suitable for data-scarce regions. Also, updated and validated landslide susceptibility maps prepared employing two different methods, which were proved effective in other regions, are helpful in choosing the best one for planning and policy-making purposes. The impact of road cuttings on slope failures in this region was not assessed by other researchers, and hence the findings of this study will be valuable reference material for researchers, engineers, geologists, and the government in preparing proper guidelines with suitable regulations for the

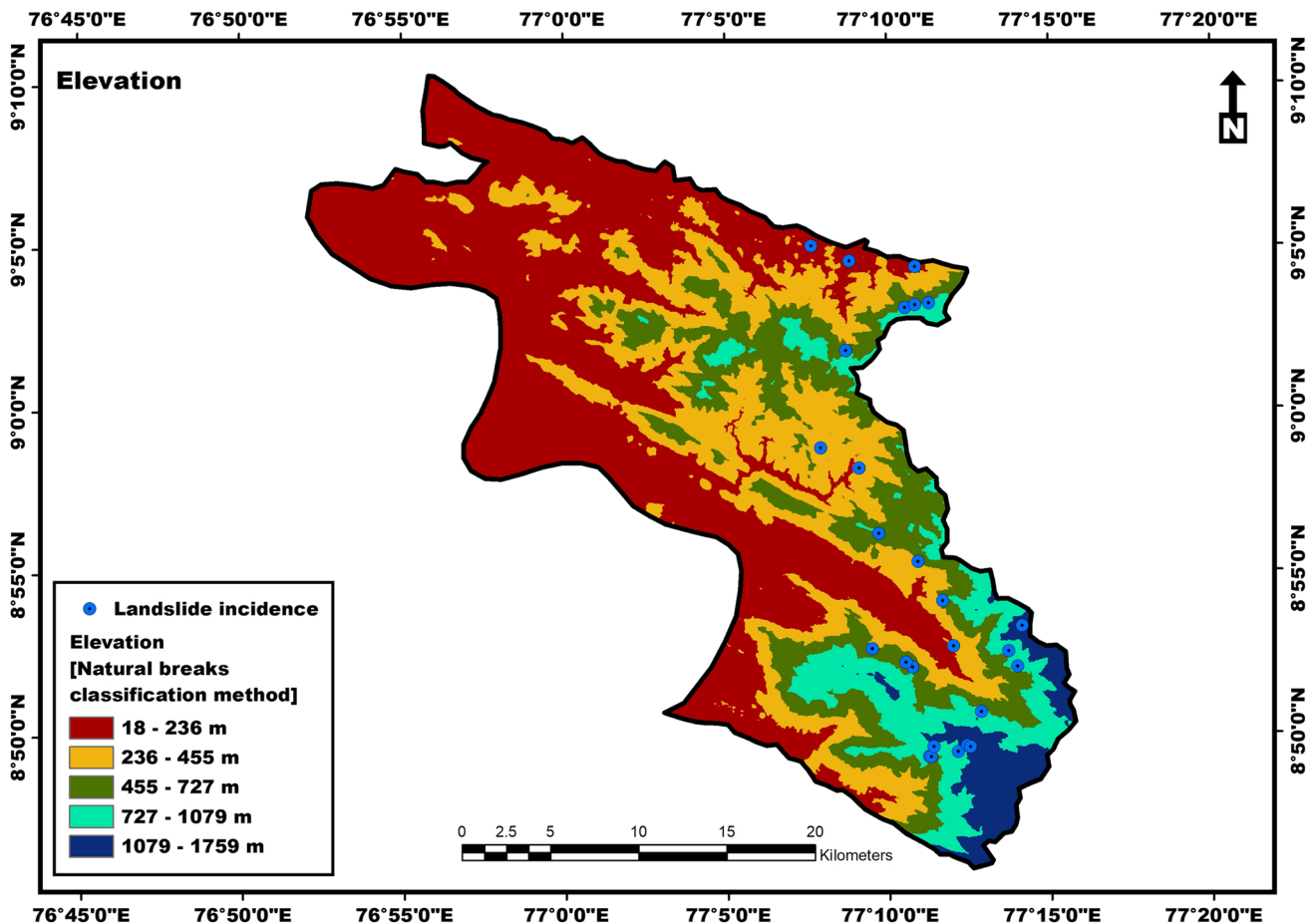


Fig. 5 Elevation

betterment of the communities. This study is intended to develop a framework to demarcate the landslide susceptible zones using GIS techniques for the Western Ghats region of Kollam district, Kerala, India, and to assess the impact of road cuttings on slope failures. For this study, ten intrinsic factors have been selected and their influence on landslide initiation will be discussed. The conditioning factors include slope angle, elevation, slope aspect, stream buffer, lithology, soil, road buffer, normalized difference vegetation index (NDVI), land use and land cover (LULC), and lineament buffer. Both the AHP and FR methods will be used to determine the weights, and the outputs will be compared to determine the prediction capability.

Materials and methods

Study area

This area is located in the southern Western Ghats (WG), a biodiversity hotspot in India (Fig. 1). It lies between

longitudes of $76^{\circ}50'0''\text{E}$ and $77^{\circ}15'0''\text{E}$ and latitudes of $8^{\circ}40'0''\text{N}$ and $9^{\circ}15'0''\text{N}$, and is around 775.18 sq. km. This area is bound by the Thiruvananthapuram district in the south, Tamil Nadu state in the east, and the Pathanamthitta district in the north. The Thenmala Dam and Reservoir are located within the study area.

Framework for the landslide susceptibility assessment

The framework for the landslide susceptibility assessment is categorized into three phases: desk studies, analysis, and field studies (Fig. 2). This framework was a modified one from Roslee et al. (2012). The literature review, data collection (satellite images, secondary data like published maps, etc.), selection of methods and factors (suitable factors will be selected based on the geo-environmental conditions of the study area, and methods will be selected based on the quality and quantity of data), and creation of landslide inventory (data on landslide affected sites will be collected from available data portals and published

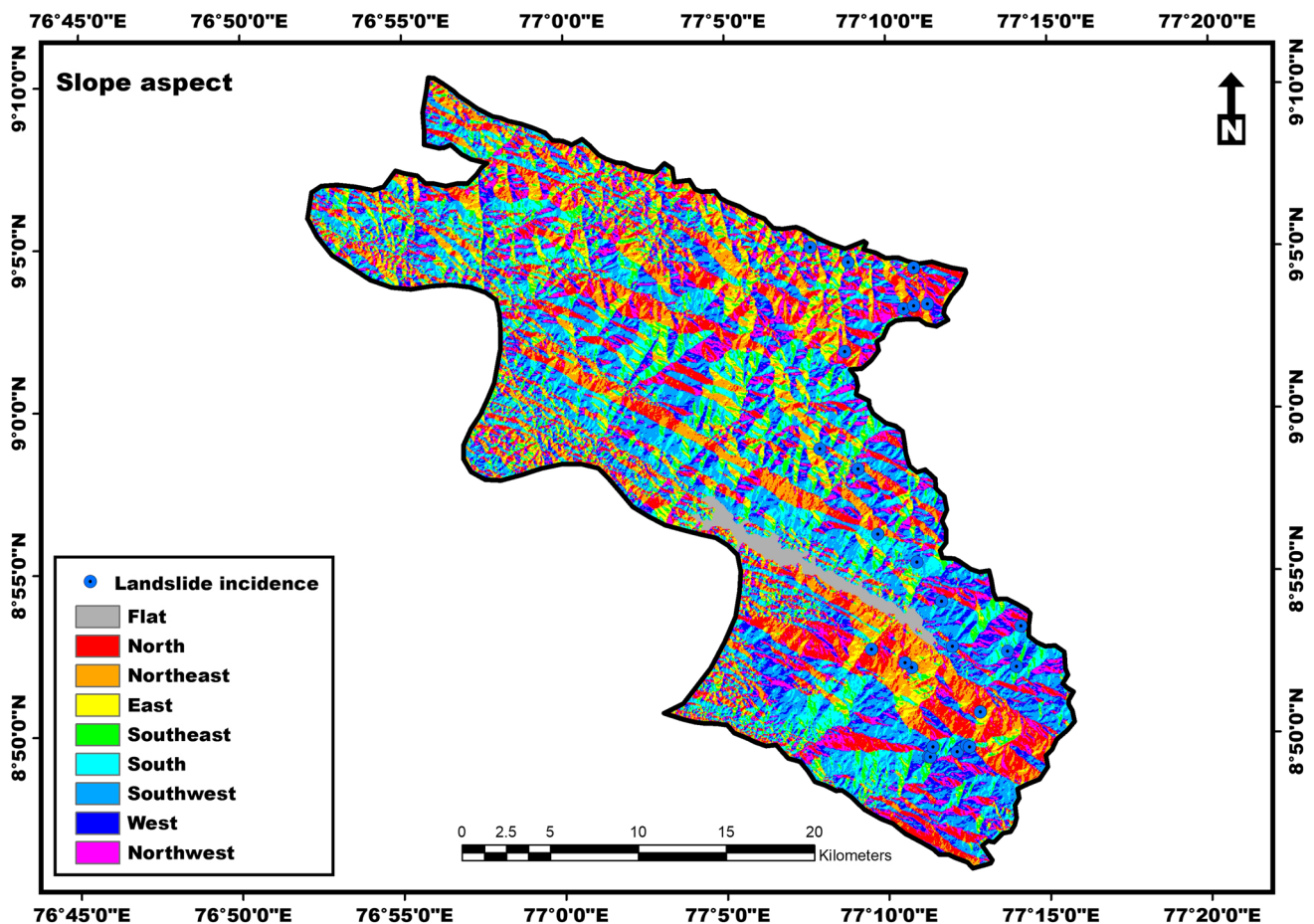


Fig. 6 Slope aspect

documents) are part of the desk studies phase. The analysis phase comprises the creation of thematic layers using the GIS software; reclassification of thematic layers and input of weights/ratings to the factor classes, input of weights derived using the methods adopted to the factors; creation of a landslide susceptibility map; classification or categorization; and validation of the susceptibility map. The field study phase comprises ground truthing of the LULC classification and collection of locations of landslide affected sites using GPS. The AHP and FR based landslide susceptibility modelling are mentioned in the following sections:

Data used

The landslide susceptibility modelling involves the following steps:

- i. The 10 conditioning factors were acquired from a variety of sources (Table 1). ArcGIS 10.4 and ERDAS

Imagine 9.2 were employed to prepare the thematic layers of these conditioning factors.

- ii. After deriving the layers, the landslide incidence data provided by the National Remote Sensing Centre (Hyderabad, India) and verified using Google Earth Pro was used as a validation dataset.
- iii. The AHP and FR models were used to produce the susceptibility maps (Fig. 3).
- iv. The ROC curve method was used to validate the created susceptibility maps. The ROC curves were created using the SPSS software.

Causative factors

Slope angle One of the most critical landslide-inducing factors is slope angle. Low gradients are often associated with reduced shear stresses, so gentle slopes should have a low landslide frequency (Akgun et al. 2008). The increase in slope angle increases the probability of the occurrence of

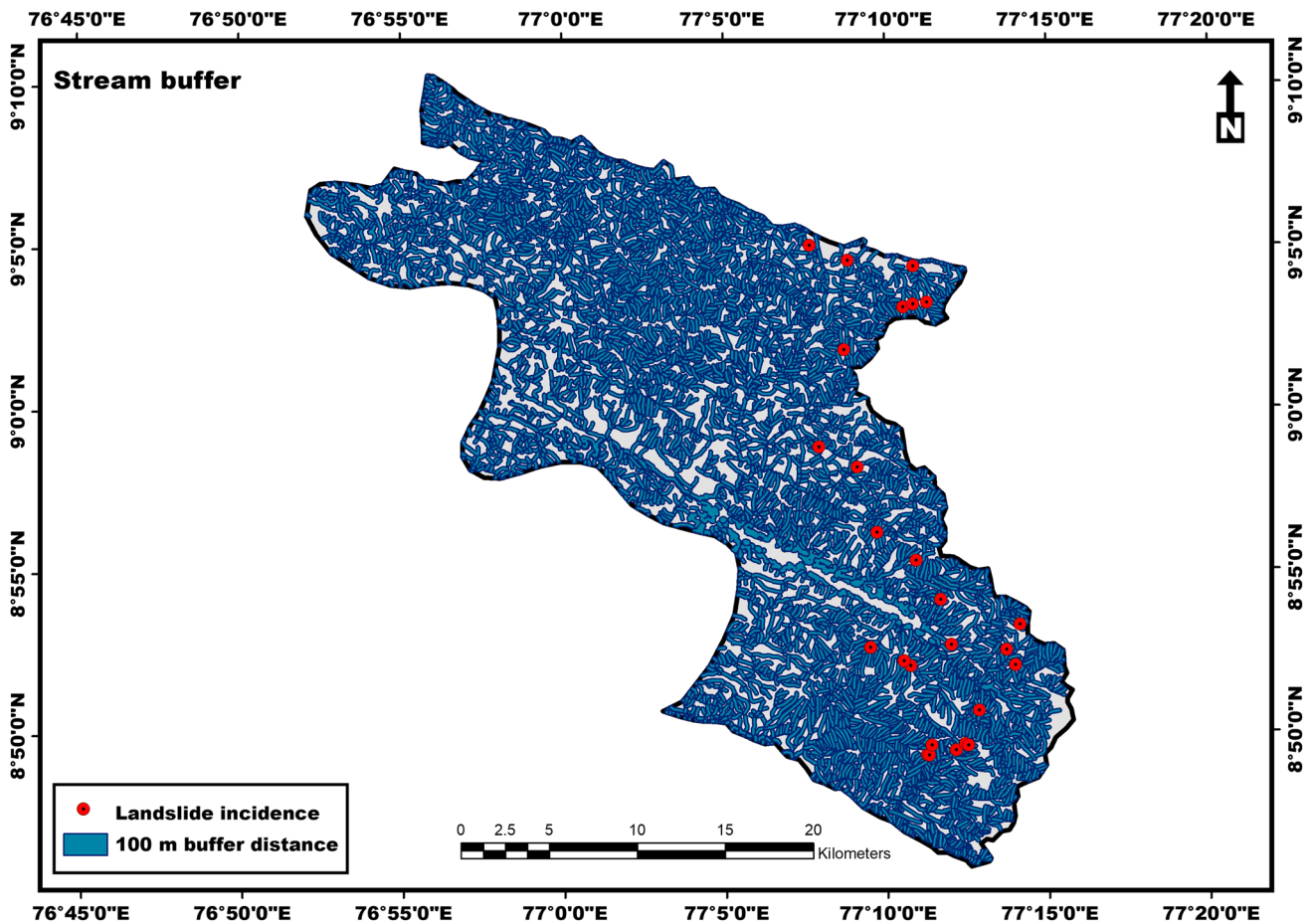


Fig. 7 Stream buffer

landslides (Achour et al. 2017), as the shear stress is directly proportional to the slope angle (Lee et al. 2004). Using ArcGIS spatial analyst (surface) tools, the slope angle was derived from the DEM. The slope (angle) of the area is categorized into 5 classes: 0–8.47°, 8.47–15.89°, 15.89–23.05°, 23.05–31.00°, and 31.00–67.57° (Fig. 4).

Elevation The probability of landslide initiation is greater at higher elevation areas (Achour and Pourghasemi 2020). The elevation was computed from the DEM using the surface tool available with ArcGIS. The elevation of the area is divided into 5 classes: 18–236 m, 236–455 m, 455–727 m, 727–1079 m, and 1079–1759 m. The elevation classes are represented in Fig. 5.

Slope aspect Slope aspect, which represents the direction of the highest slope of the terrain (Xu et al. 2012), is another important factor used in stability assessment of hillslopes. The solar influences are greater on the southern and western aspects (Setiawan et al. 2004), and these slopes have

less vegetation density and are subjected to a higher rate of erosion (Elmoulat and Ait Brahim 2018). Erosion is further accelerated by the higher intensity of rainfall. The westward and south-westward slopes are more vulnerable to soil erosion since the wind blowing from these directions brings more rain than the wind from the east (Beullens et al. 2014), making these slopes more susceptible to landslides. The slope aspect was extracted from the DEM employing ArcGIS surface tools, and is grouped into nine (Fig. 6).

Stream buffer Landslides can be triggered by terrain alteration induced by gully erosion (Pradhan et al. 2010b). Streams can wreak havoc on the stability of slope materials by undercutting or saturating them, lowering their shear resistance (Dai et al. 2001; Saha et al. 2002). Therefore, the areas closer to stream channels are more vulnerable to landslides. The stream networks of the study area were digitized from the topographic maps and a 100 m buffer distance was derived using spatial analyst tools (Fig. 7).

Lithology The strength and permeability of rock depend on the rock type (Achour et al. 2017), the degree of weathering,

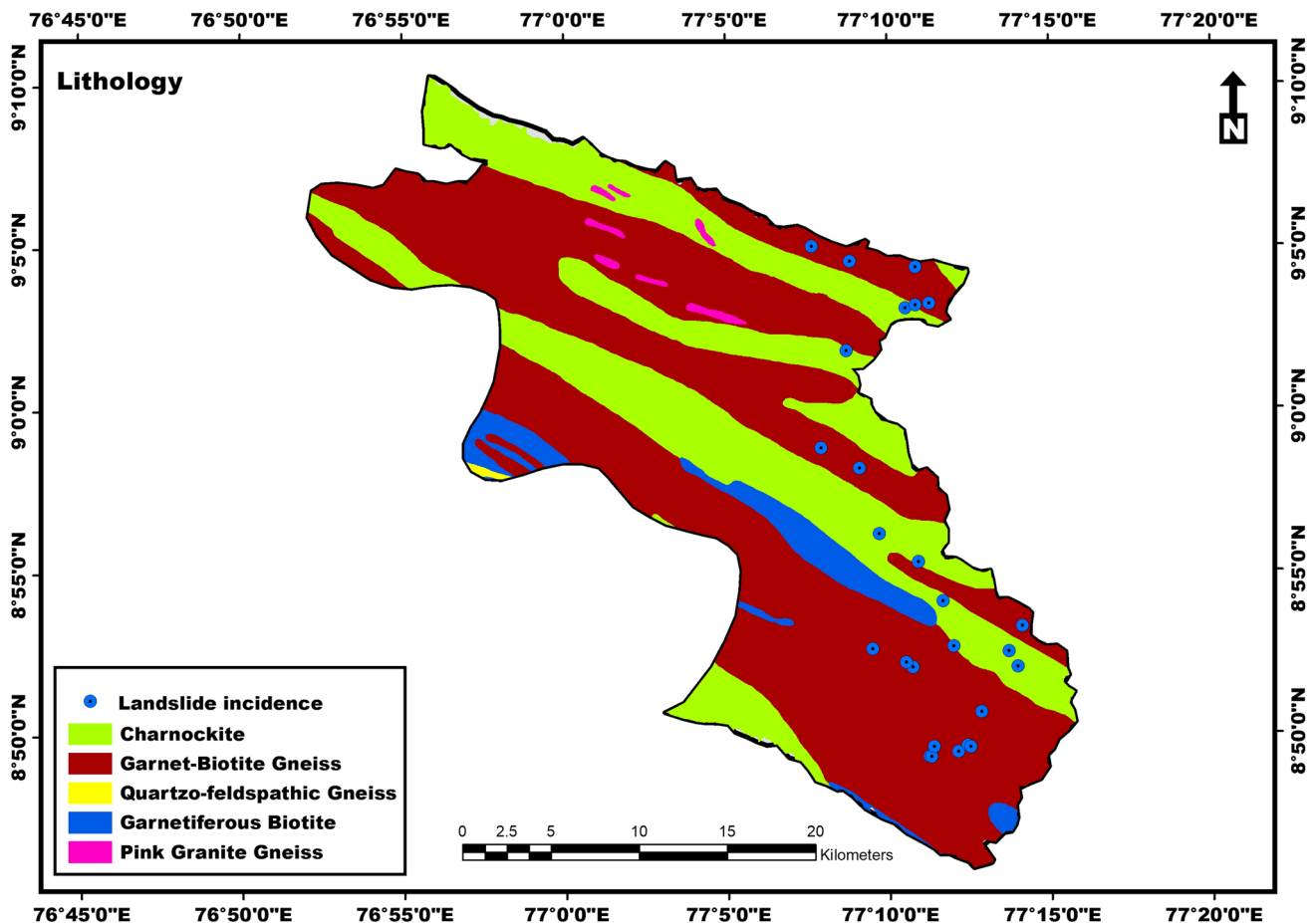


Fig. 8 Lithology

as well as the presence and type of discontinuities (such as joints or fractures) (Ajin et al. 2016). Stronger rocks are less susceptible to landslides because they are more resistant to the driving forces (Kanungo et al. 2006). The lithology was extracted from the geological map using ArcGIS tools. The rocks (Fig. 8) present in this region includes charnockite, garnet-biotite gneiss with migmatite, garnetiferous biotite, pink granite gneiss, and quartzo-feldspathic gneiss.

Soil Soils in the Western Ghats with higher clay content typically have high porosity and low permeability, so they can hold more water. The shear strength of soil gets much reduced when the water pressure in the pores increases; this leads to slope failures (Chawla et al. 2018). Landslides are influenced by the presence of clayey soil, which functions as a potential slip zone (Sartohadi et al. 2018). The soil texture of this area was extracted from the soil map using ArcGIS tools (Fig. 9).

Road buffer Road cuts are sites of anthropogenic instability (Pradhan et al. 2010b). The slope equilibrium can be affected by excavation for road construction and increased

loads due to vehicle movements (Pourghasemi et al. 2012b). The shear strength at the slope’s toe can be reduced by road cuts (Semlali et al. 2019) and can result in landslides. The topographic maps were used to digitize the road networks, which were then updated using Google Earth Pro data. A 100 m buffer distance was derived using ArcGIS spatial analyst tools (Fig. 10).

Normalized difference vegetation index NDVI quantifies the vegetation density was derived from the satellite image using the ArcGIS raster calculator tool. NDVI was derived using Eq. 1 (Rouse et al. 1974) and ranges between -1 and $+1$. Higher NDVI (close to $+1$) represents dense vegetation, whereas lower NDVI represents sparse vegetation. The NDVI less than zero indicates water and NDVI close to zero indicates bare land, rock or urbanized areas (Saravanan et al. 2019; Viana et al. 2019). The probability of landslide occurrence is higher in areas with lower NDVI (sparse vegetation). The NDVI of this area (Fig. 11) is categorized into five ($-0.06-0.10$, $0.10-0.26$, $0.26-0.32$, $0.32-0.38$, and $0.38-0.63$).

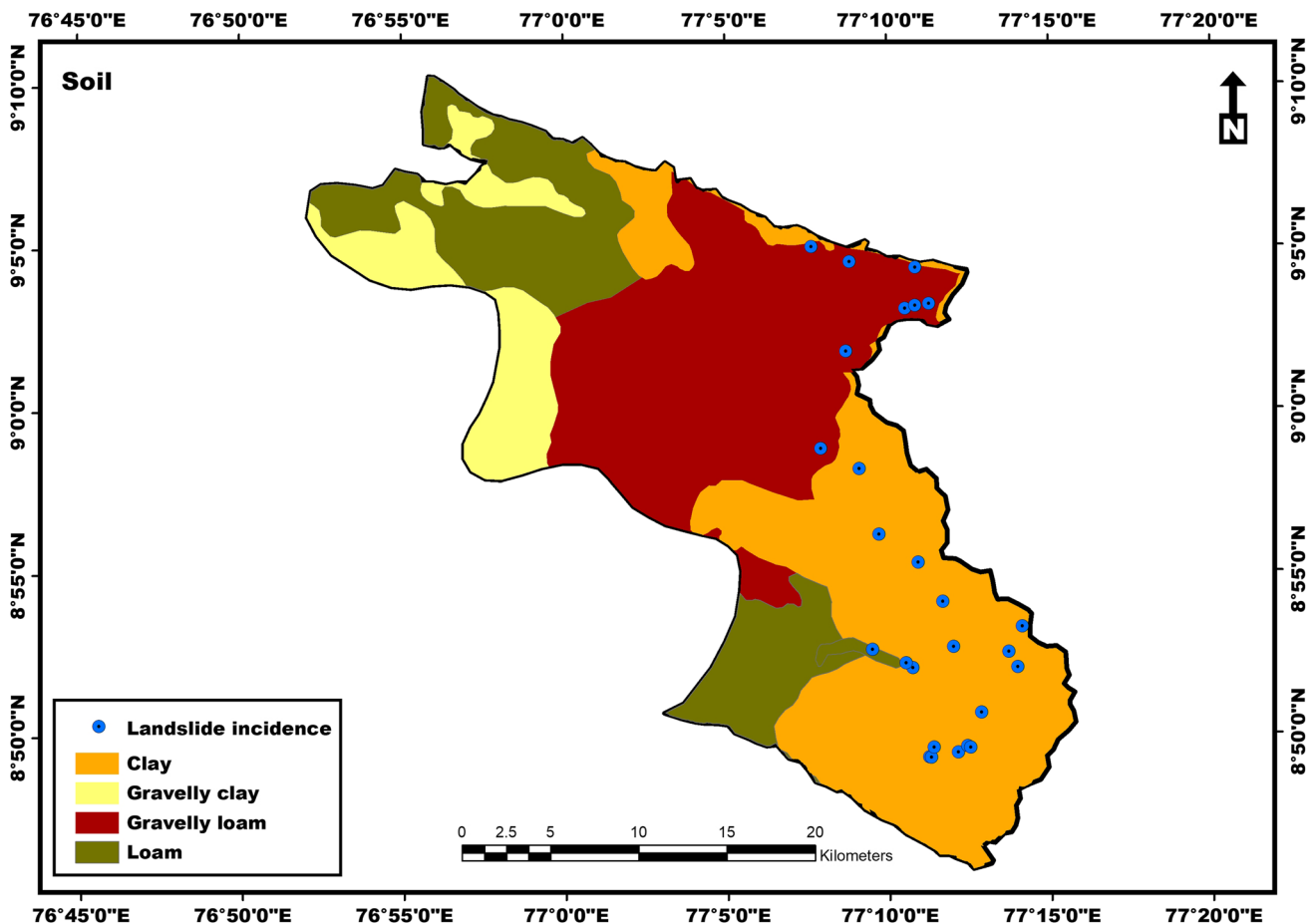


Fig. 9 Soil

$$NDVI = \frac{(NIR - R)}{(NIR + R)} \quad (1)$$

where NIR and R stand for spectral reflectance measurements acquired in the near-infrared and visible regions, respectively.

Land use and land cover Areas with thicker vegetation are less prone to landslides. This is due to the fact that vegetation with their root systems can stabilize the slopes (García-Rodríguez et al. 2008) by binding the soil particles, which increases soil shear strength (Turrini and Visintainer 1998). The sparsely vegetated or barren areas are more prone to sliding as these areas are subjected to weathering (Anbalagan 1992). Changes in the land cover on hill slopes can induce slope failures (Kanungo et al. 2009; Karsli et al. 2009). The land use and land cover types were derived from the Landsat image. The maximum likelihood (ML) classification (Mohajane et al. 2018) tool available in the ERDAS Imagine was applied to categorize the satellite image. The land use and land cover types (Fig. 12) of this area include

agricultural land, evergreen forest, deciduous forest, barren land, water bodies, built-up areas, scrubland, and mixed vegetation.

Lineament buffer Along faults, landslides are more common (Semlali et al. 2019). These tectonic breaks can decrease the strength of rocks (Devkota et al. 2013). Lineaments initiate the weathering process and thus disintegrate and decompose the rocks (Mandal and Maiti 2014). Under saturated conditions, these weathered materials may lose their consistency and initiate sliding. The lineaments were downloaded from the Bhukosh portal and the 100 m buffer distance was calculated using spatial analyst tools (Fig. 13).

AHP modeling

The AHP model was developed by Saaty (1980) and is the most widely used technique for decision making in complicated contexts where numerous variables or criteria are taken into account while prioritizing and selecting alternatives. In the AHP modelling, a 1–9 scale is used to

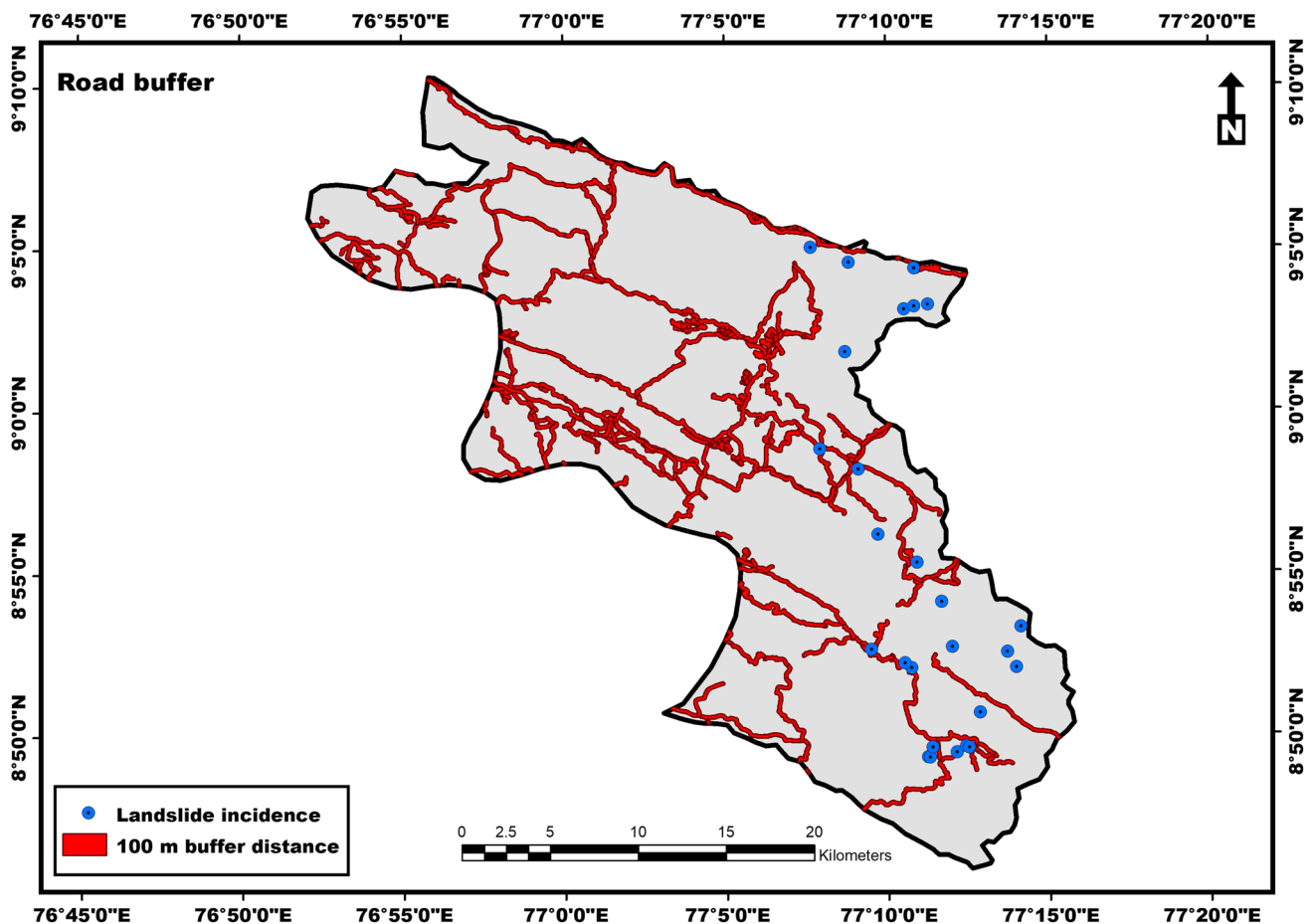


Fig. 10 Road buffer

construct judgement matrices (Saaty 1980). The crucial processes involved in the modelling are the creation of a pairwise comparison matrix (Table 2), the estimation of Eigen value, Eigen vector, and weighting coefficient (Table 3), and the estimation of the consistency ratio (Table 4) to check the consistency (Nikhil et al. 2021).

The Eigen vector (Vp), and weighting coefficient (Cp) were determined applying Eqs. 2 and 3 as in Nikhil et al. (2021)

$$V_p = \sqrt[k]{W_1 \times \dots \times W_k} \tag{2}$$

Where k = number of factors; W = ratings of the factors.

$$C_p = \frac{V_p}{V_{p1} + \dots + V_{pk}} \tag{3}$$

The matrix normalization, calculation of priority vector [C], overall priority [D], rational priority [E] were done as in Nikhil et al. (2021).

The Eigen value (λ_{max}), consistency index (CI), and consistency ratio (CR) were determined using Eqs. 4 and 5 as in Nikhil et al. (2021)

$$\lambda_{max} = \frac{[E]}{k} \tag{4}$$

$$CI = (\lambda_{max} - k)/(k - 1) \tag{5}$$

$$CR = \frac{CI}{RI} \tag{6}$$

where RI = random index (Saaty 1980).

Saaty (1980) suggests that the CR should be less than 0.1 (i.e., 10%), otherwise the judgements are unreliable and we need to revise the subjective judgements. Hence, the judgements are acceptable in this study because the CR is 0.040 (which is less than 0.1).

The weights obtained from the AHP modelling is shown in Eq. 7.

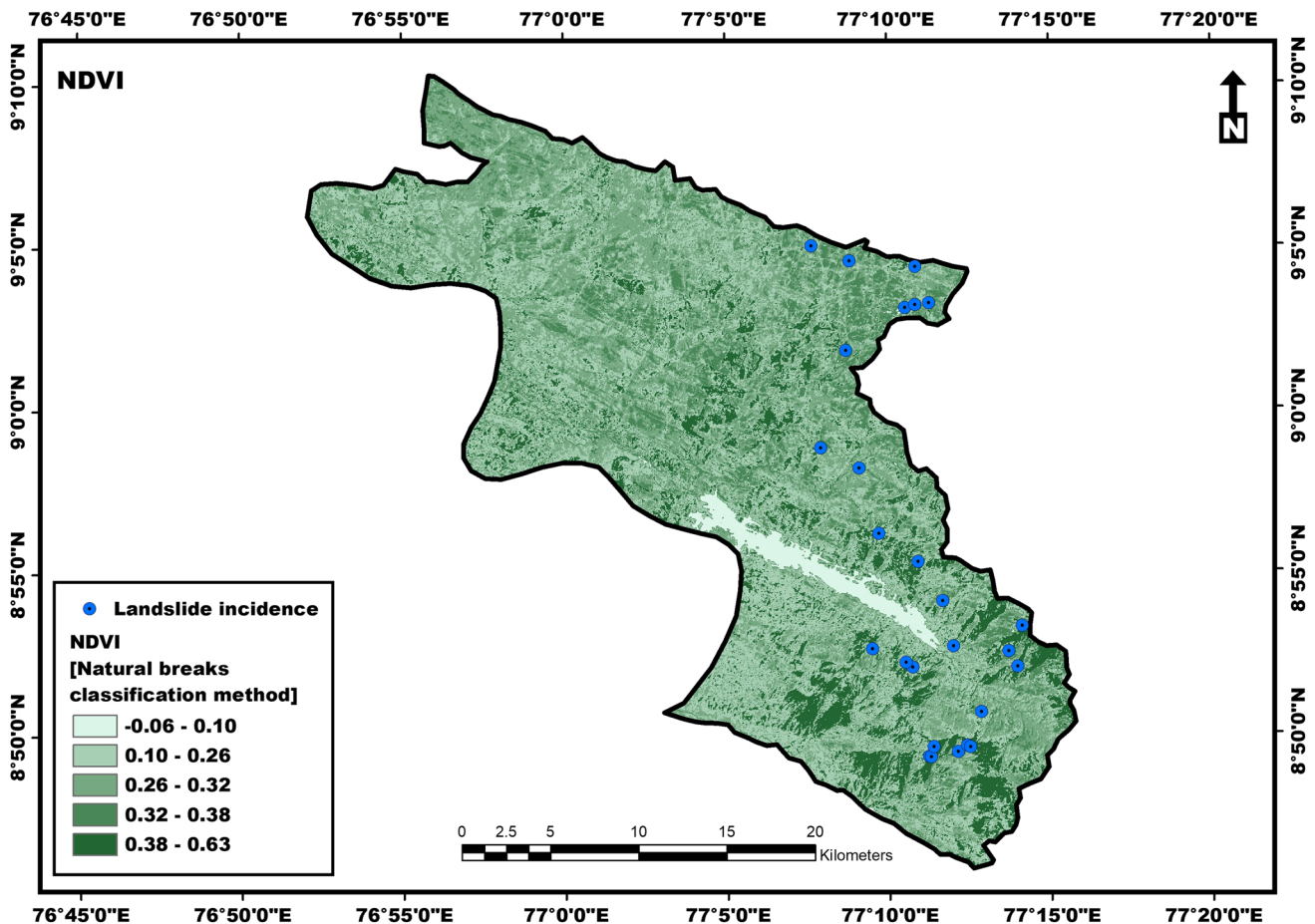


Fig. 11 Normalized difference vegetation index

$$\begin{aligned}
 \text{LSZ} = & (0.291 \times \text{Slp.}) + (0.216 \times \text{Ele.}) \\
 & + (0.155 \times \text{Asp.}) + (0.110 \times \text{SB}) \\
 & + (0.077 \times \text{Litho.}) + (0.054 \times \text{Soil}) \\
 & + (0.038 \times \text{RB}) + (0.027 \times \text{NDVI}) \\
 & + (0.019 \times \text{LULC}) + (0.014 \times \text{LB})
 \end{aligned}
 \tag{7}$$

$$\begin{aligned}
 \text{LSZ} = & Fr(\text{Slp.}) + Fr(\text{Ele.}) + Fr(\text{Asp.}) + Fr(\text{SB}) \\
 & + Fr(\text{Litho.}) + Fr(\text{Soil}) + Fr(\text{RB}) + Fr(\text{NDVI}) \\
 & + Fr(\text{LULC}) + Fr(\text{LB})
 \end{aligned}
 \tag{8}$$

FR modelling

The FR is the proportion of landslides in a desired class as a percentage of all landslides to the class’s area as a percentage of the total study area (Silalahi et al. 2019). A lower FR value (< 1) implies a lower level of landslide susceptibility, whereas a larger FR value (> 1) suggests a higher level of landslide susceptibility (Silalahi et al. 2019). The FR of each factor and its classes is included in Table 5. The susceptible zones were created by applying Eq. 8.

Validation of the results – ROC curve method

The performance of a classifier is evaluated using ROC curves, with sensitivity plotted on the Y-axis and 1-specificity plotted on the X-axis (Grimnes and Martinsen 2015). The AUC, or area under the receiver operating characteristic (ROC) curve, is a single scalar value that quantifies performance of a binary classifier (Hanley and McNeil 1982). AUC values of 0.5 imply no discrimination, 0.7 to 0.8 are acceptable, 0.8 to 0.9 are excellent, and greater than 0.9 are outstanding (Hosmer and Lemeshow 2000). There was a total of 26 landslides recorded in the study area, which were used for validation. The SPSS 25 software was utilized for plotting the ROC graph and estimating the AUC values.

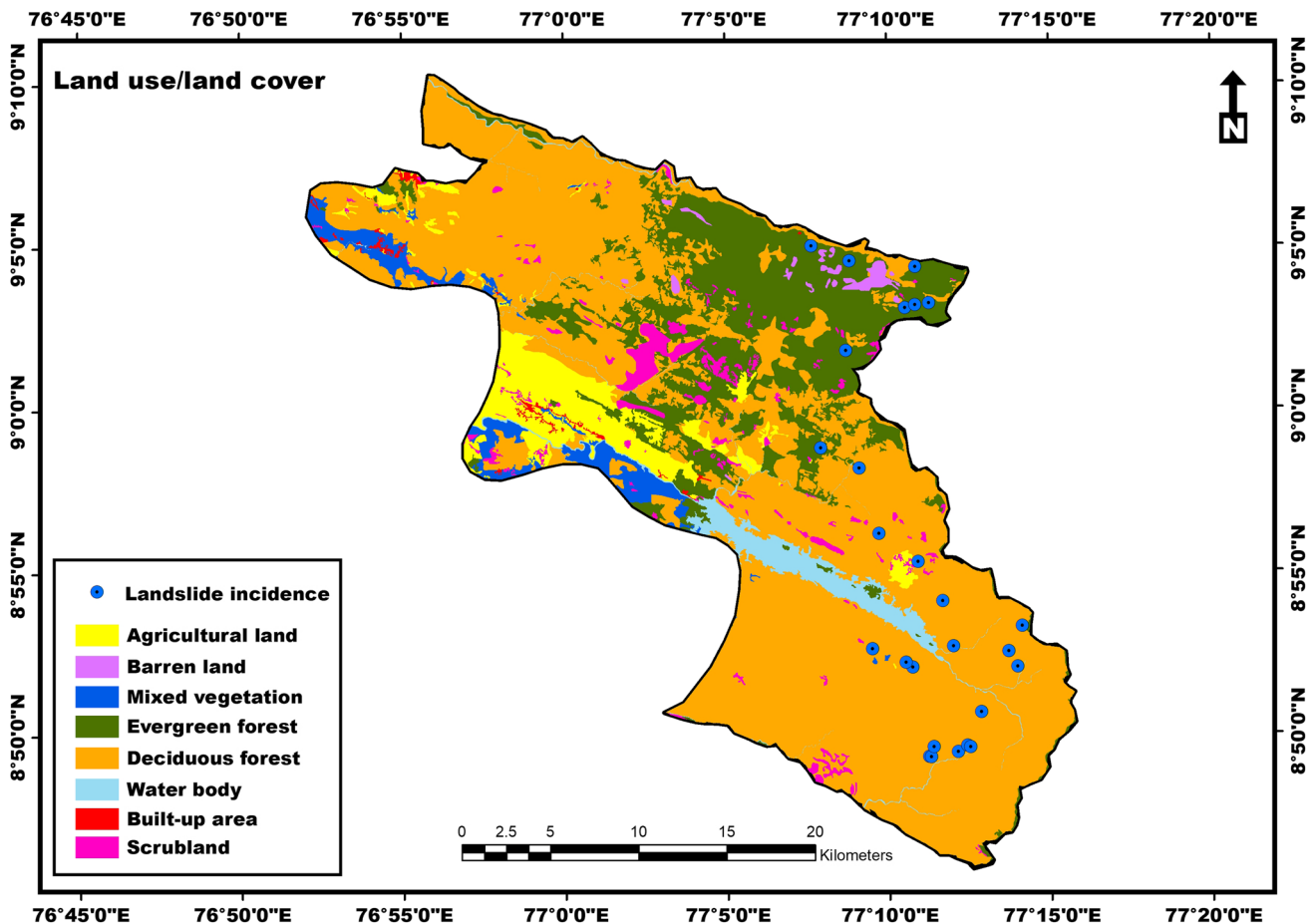


Fig. 12 Land use/land cover types

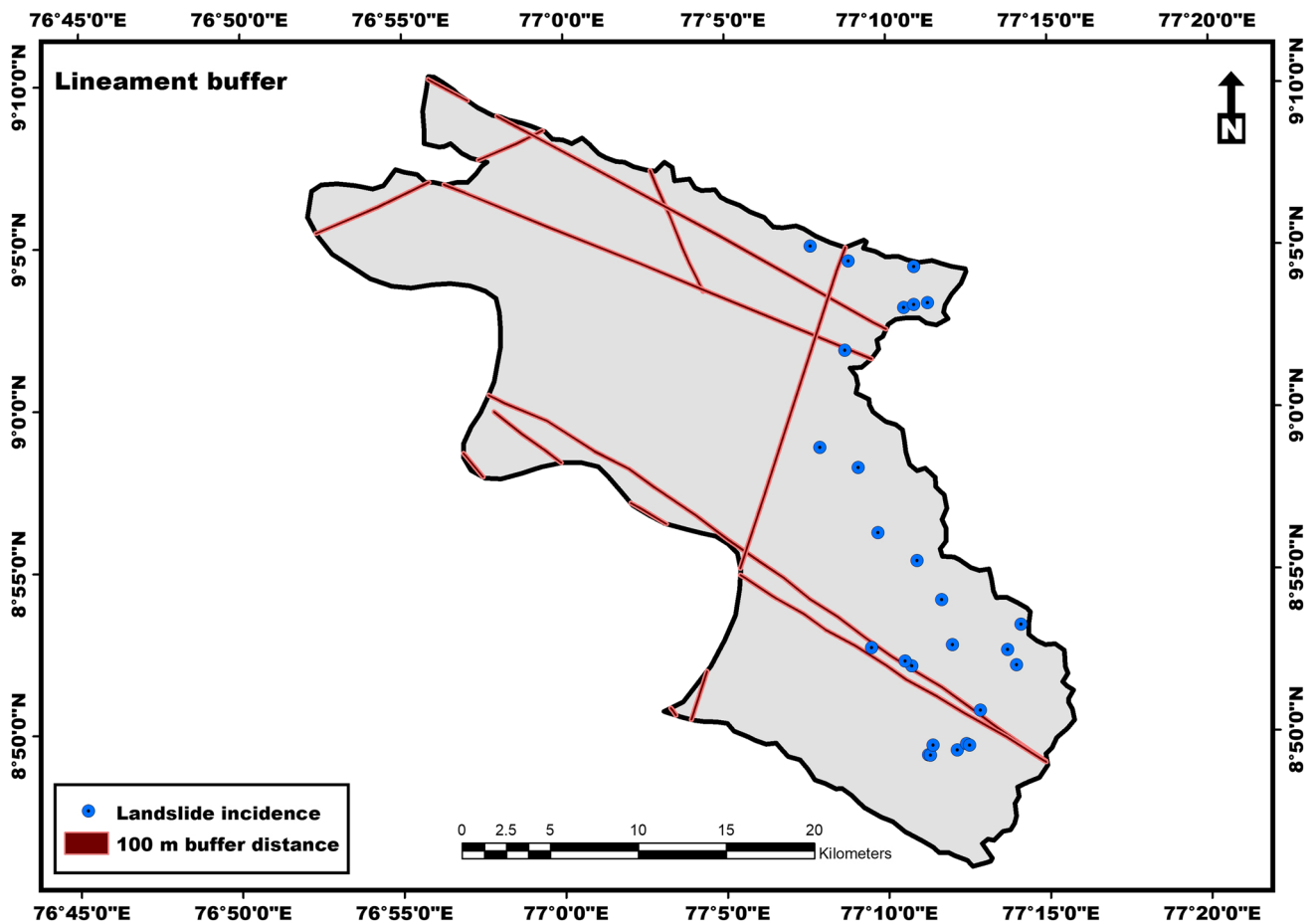


Fig. 13 Lineament buffer

Results and discussion

In this study, the AHP and FR models and GIS were applied to determine the susceptibility of the Western Ghats region

in Kollam district. Ten causative factors, viz. slope angle, elevation, slope aspect, stream buffer, lithology, soil, road buffer, NDVI, LULC, and lineament buffer, were used for susceptibility modeling. Based on the level of susceptibility,

Table 2 Pairwise comparison matrix

	Slp.	Ele.	Asp.	SB	Litho.	Soil	RB	NDVI	LULC	LB	Vp	Cp
Slp.	1	2	3	4	5	6	7	8	9	10	4.529	0.291
Ele.	1/2	1	2	3	4	5	6	7	8	9	3.356	0.216
Asp.	1/3	1/2	1	2	3	4	5	6	7	8	2.414	0.155
SB	1/4	1/3	1/2	1	2	3	4	5	6	7	1.707	0.110
Litho.	1/5	1/4	1/3	1/2	1	2	3	4	5	6	1.196	0.077
Soil	1/6	1/5	1/4	1/3	1/2	1	2	3	4	5	0.836	0.054
RB	1/7	1/6	1/5	1/4	1/3	1/2	1	2	3	4	0.586	0.038
NDVI	1/8	1/7	1/6	1/5	1/4	1/3	1/2	1	2	3	0.414	0.027
LULC	0	1/8	1/7	1/6	1/5	1/4	1/3	1/2	1	2	0.295	0.019
LB	0	1/9	1/8	1/7	1/6	1/5	1/4	1/3	1/2	1	0.221	0.014
SUM	2.92	4.83	7.72	11.59	16.45	22.28	29.08	36.83	45.50	55.00	15.55	1.00

Where Slp. = Slope; Ele. = Elevation; Asp. = Aspect; SB = Stream buffer; Litho. = Lithology; RB = Road buffer; LB = Lineament buffer

Table 3 Normalized matrix

	Slp.	Ele.	Asp.	SB	Litho.	Soil	RB	NDVI	LULC	LB	Rank
Slp.	0.34	0.41	0.39	0.35	0.30	0.27	0.24	0.22	0.20	0.18	2.90
Ele.	0.17	0.21	0.26	0.26	0.24	0.22	0.21	0.19	0.18	0.16	2.10
Asp.	0.11	0.10	0.13	0.17	0.18	0.18	0.17	0.16	0.15	0.15	1.52
SB	0.09	0.07	0.06	0.09	0.12	0.13	0.14	0.14	0.13	0.13	1.09
Litho	0.07	0.05	0.04	0.04	0.06	0.09	0.10	0.11	0.11	0.11	0.79
Soil	0.06	0.04	0.03	0.03	0.03	0.04	0.07	0.08	0.09	0.09	0.56
RB	0.05	0.03	0.03	0.02	0.02	0.02	0.03	0.05	0.07	0.07	0.40
NDVI	0.04	0.03	0.02	0.02	0.02	0.01	0.02	0.03	0.04	0.05	0.28
LULC	0.03	0.03	0.02	0.01	0.01	0.01	0.01	0.01	0.02	0.04	0.20
LB	0.03	0.02	0.02	0.01	0.01	0.01	0.01	0.01	0.01	0.02	0.15
Total	1.00	1.00	1.00	1.00	1.00	1.00	1.00	1.00	1.00	1.00	10.00

the study area is divided into five zones, as shown in Table 6. The landslide-susceptible zone maps are shown in Figs. 14 and 15. During the 2018 southwest monsoon, a total of 26 landslides occurred in this region. The ROC curve analysis confirmed the outstanding AUC value (above 0.90) for the susceptibility maps produced using the AHP (0.906) and FR (0.926) models, respectively (Fig. 16). The higher AUC value for the FR model confirmed that FR has a better prediction accuracy than the AHP model in demarcating landslide susceptible zones. The high and very high susceptibility zones together constitute 33.3% and 23.59% of the study area in the maps produced using the AHP and FR models, respectively. The study by Thomas et al. (2021) also found that the FR model is more efficient than the AHP model in susceptibility zonation of landslides.

Most of the critical areas were observed in areas with a higher slope angle. The areas with higher slope angles are generally unstable. The FR values of 1.39 and 3.94 for slopes ranging from 23.05 to 31.00° and 31.00 to 67.57°, respectively, confirmed the role of steeper slopes in slope failures. The study by Yang et al. (2015) also confirmed

higher landslide incidences at slopes ranging between 30 and 40°. The majority of the slope failures were observed in high elevation regions and also in areas bordering moderate and higher elevation regions. The FR value (3.29) confirmed that the elevation ranging between 727 and 1079 m has a higher correlation with landslide occurrence. In their study, Shao et al. (2020) found steeper slopes with higher elevations to be ideal sites for landslide occurrence. The number of landslide incidences was found to be high (18 landslides) in close proximity to stream channels. This is due to increased saturation conditions, stream bank erosion, or toe cutting due to river flow. The rock types present in the study area belong to the crystalline group. And the number of landslide incidences was found to be high in garnet-biotite gneiss rocks (with a FR value of 1.12). A study by Thomas et al. (2021) also found higher landslide incidences in gneissic terrain. Areas with clayey soils are potential slip zones. This was confirmed by assessing the number of landslide incidences in the areas with clayey soils. A total of 17 landslide incidences (with a FR value of 1.71) occurred in areas with clayey soil. Thomas et al. (2021) also reported

Table 4 Consistency ratio

	[C]	[D] = [A]x[C]	[E] = [D]/[C]	λ_{max}	CI	CR
Slp.	0.290	3.175	10.942	10.530	0.059	0.039
Ele.	0.210	2.320	11.048			
Asp.	0.152	1.666	10.993			
SB	0.109	1.183	10.811			
Litho	0.079	0.832	10.563			
Soil	0.056	0.582	10.315			
RB	0.040	0.406	10.129			
NDVI	0.028	0.286	10.056			
LULC	0.020	0.203	10.156			
LB	0.015	0.156	10.282			
SUM	1.000		105.296			

Table 5 Frequency ratio of factors

Thematic layer	Class	Number of pixels in the class	Class (%)	Number of landslides incidence points within the class	Landslide incidence points (%)	Frequency ratio
Slope angle	0–8.47	181,118	21.80	1	3.85	0.17
	8.47–15.89	222,801	26.83	6	23.07	0.86
	15.89–23.05	202,043	24.32	4	15.38	0.63
	23.05–31.00	159,849	19.25	7	26.93	1.39
	31.00–67.57	64,829	7.80	8	30.77	3.94
Elevation (m)	18–236	375,947	45.26	4	15.38	0.34
	236–455	204,504	24.62	2	7.69	0.31
	455–727	136,224	16.40	9	34.62	2.11
	727–1079	77,665	9.35	8	30.77	3.29
	1079–1759	36,300	4.37	3	11.54	2.64
Slope aspect	Flat	17,367	2.09	0	0	0
	North	125,420	15.11	0	0	0
	Northeast	106,436	12.81	7	26.92	2.10
	East	62,114	7.48	0	0	0
	Southeast	64,472	7.76	5	19.23	2.47
	South	111,145	13.38	6	23.08	1.72
	Southwest	157,158	18.92	3	11.54	0.61
	West	101,095	12.17	2	7.69	0.63
Stream buffer (m)	Northwest	85,433	10.28	3	11.54	1.12
	≤ 100	549,053	66.10	18	69.24	1.04
	> 100	281,587	33.90	8	30.76	0.90
Lithology	Charnockite	274,111	33.00	8	30.76	0.93
	Quartzo-feldspathic gneiss	997	0.12	0	0	0
	Pink granite gneiss	5233	0.63	0	0	0
	Garnetiferous biotite	37,961	4.57	0	0	0
	Garnet-biotite gneiss	512,338	61.68	18	69.24	1.12
Soil	Clay	317,553	38.23	17	65.39	1.71
	Gravelly clay	81,070	9.76	0	0	0
	Gravelly loam	272,035	32.75	8	30.76	0.93
	Loam	159,982	19.26	1	3.85	0.20
Road buffer (m)	≤ 100	99,012	11.92	5	19.23	1.61
	> 100	731,628	88.08	21	80.77	0.91
NDVI	-0.06–0.10	20,683	2.49	0	0	0
	0.10–0.26	91,370	11.00	5	19.23	1.74
	0.26–0.32	285,325	34.35	6	23.08	0.67
	0.32–0.38	304,929	36.71	6	23.08	0.62
	0.38–0.63	128,333	15.45	9	34.61	2.24
Land use/land cover	Agricultural land	53,327	6.42	0	0	0.00
	Barren land	5317	0.64	0	0	0
	Built-up area	3322	0.40	0	0	0
	Mixed vegetation	25,585	3.08	0	0	0
	Deciduous forest	536,676	64.61	18	69.24	1.07
	Evergreen forest	156,575	18.85	8	30.76	1.63
	Water bodies	26,580	3.20	0	0	0
	Scrubland	23,258	2.80	0	0	0
Lineament buffer (m)	≤ 100	33,890	4.08	0	0	0
	> 100	796,749	95.92	26	100	1.04

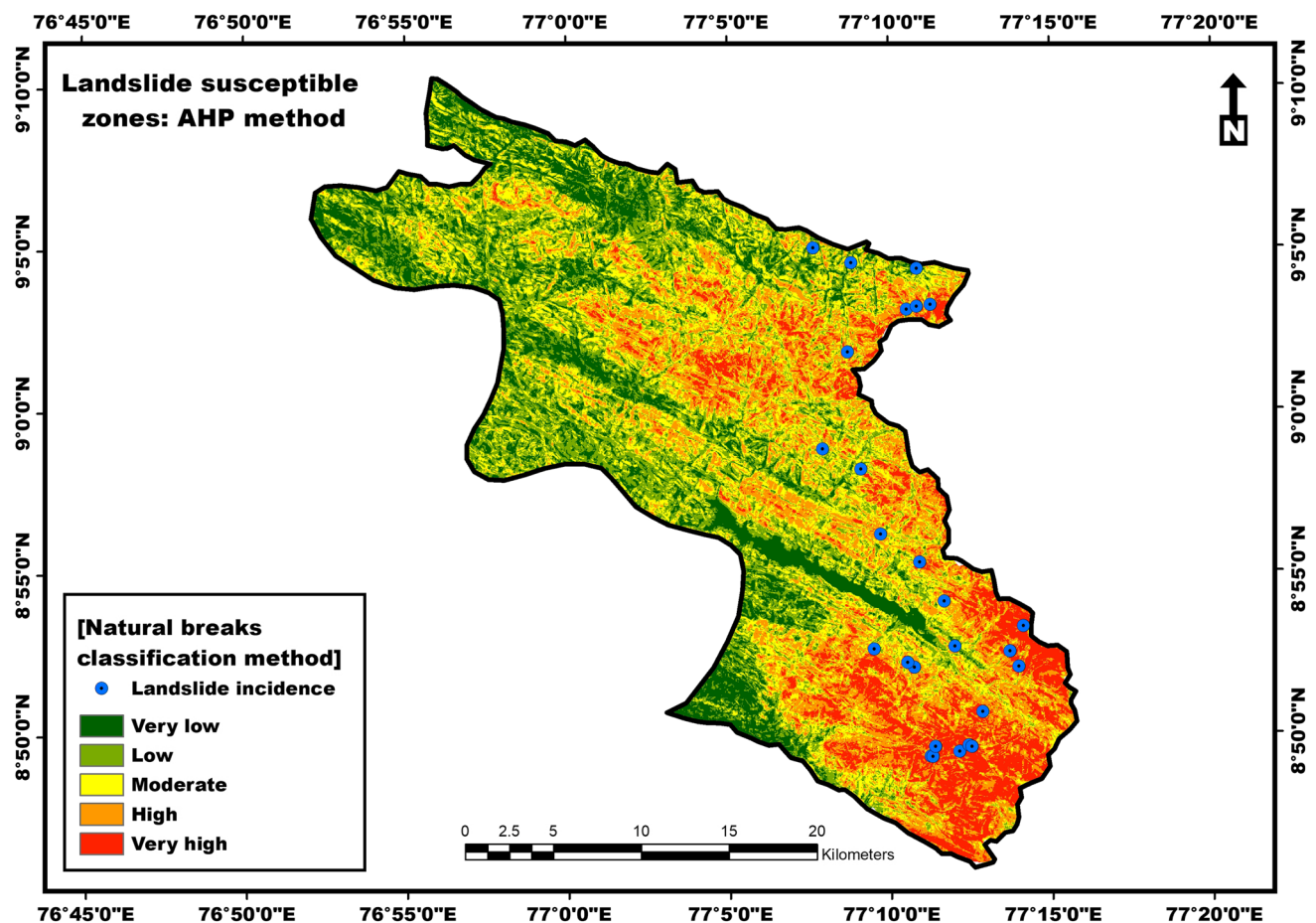


Fig. 14 Landslide susceptible zones – AHP method

that the majority of landslide incidences (91.35%) have been recorded in the areas with clayey soil. A considerable number of landslides occurred along road cuttings with a FR value of 1.61. Road cuttings can destabilize the slopes by reducing the shear strength of the toe. The occurrence of failures along the road cuttings is evidence of their anthropogenic origin. A study conducted by Sujatha and Sridhar (2021) in Connoor found that about 74% of the landslides induced as a result of road cuttings.

Applying the Fuzzy-AHP model, Sur et al. (2020) created landslide susceptibility zones along a road corridor in the Himalayan region (Kalsi-Chakrata Road corridor), which were frequently affected by landslides. They found 55% of the area to be in very high and high landslide susceptibility zones. Panchal and Shrivastava (2021) created a landslide hazard zone map of National Highway 5 in India employing the AHP model, where they found 21.56% of the area as a very high hazard zone. The study by Getachew and Meten (2021) found road cuttings as one of the crucial reasons

for the landslide occurrence in the Kabi-Gebro locality of Ethiopia. The study conducted by Tien et al. (2021) along the Halong-Vandon Expressway in Quang Ninh Province (Vietnam) found that out of 44 landslides recorded during June - August (in the years 2017 and 2018), 35 were shallow debris flows. They found that moderate to high intensity short-period rainfall is the triggering (extrinsic) factor, and that slope cutting for road developments is the major conditioning/causative factor for landslide occurrence.

The shallow slope failures occurring in this area can be minimized by applying nature-based solutions (NbS). When compared to grey engineering solutions, NbS is effective in preventing shallow slope failures (Arce-Mojica et al. 2019) and cost-effective (Chausson et al. 2020; Reguero et al. 2018; Singh et al. 2020). Rahardjo et al. (2014) assessed the performance of both Orange Jasmin and Vetiver grass in reducing slope stability. They found both shrubs effective in minimizing rainfall infiltration on a slope in Singapore. Mohammed et al. (2018) used grasses like Cynodon

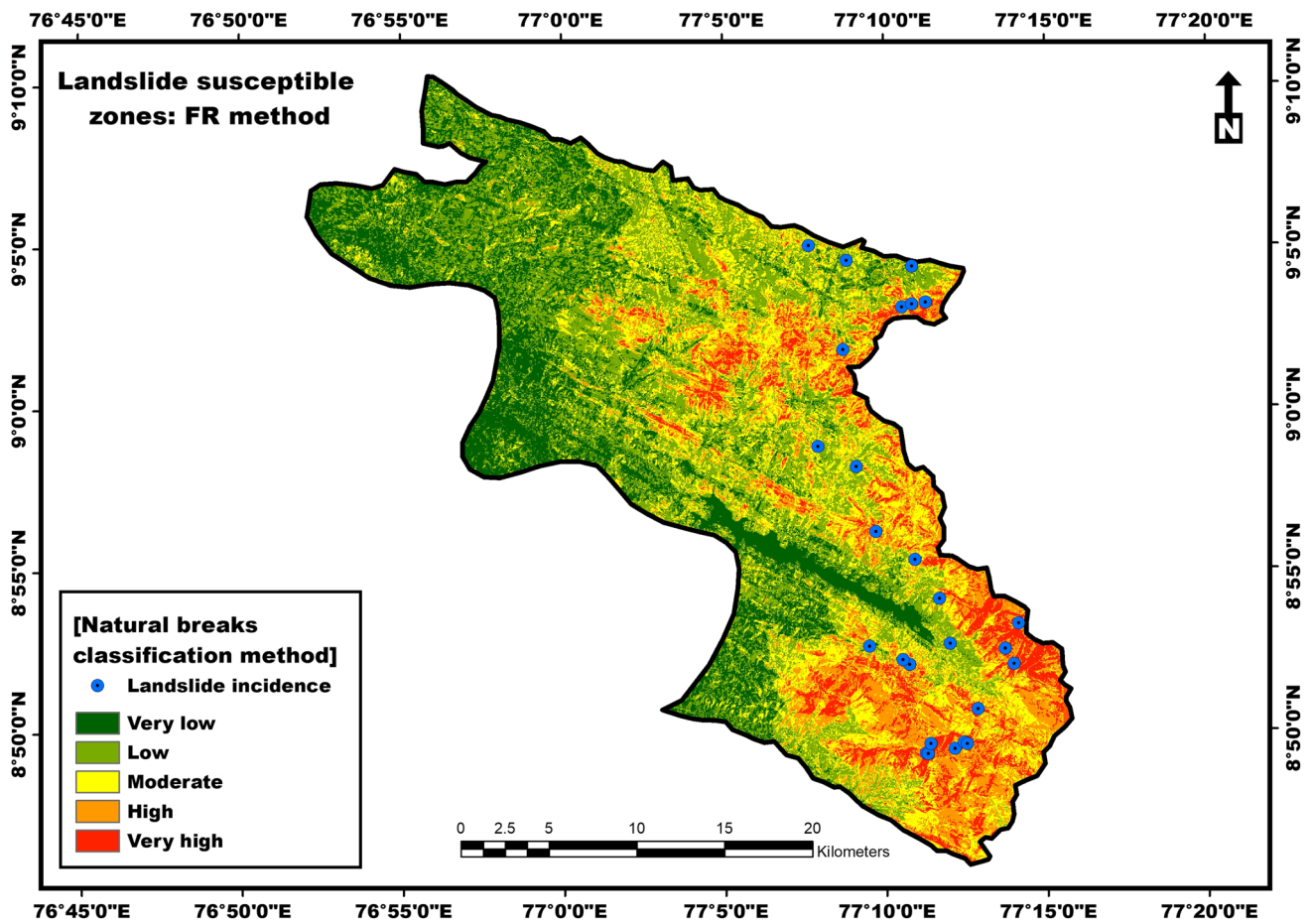


Fig. 15 Landslide susceptible zones – FR method

dactylon and Vetiver for stabilizing a slope along the Wad Medani-Sennar road in Sudan, and found it an excellent solution. Gobinath et al. (2015) found that using lemon grass roots to stabilise landslide-affected soils in the Nilgiri district of India increased shear strength while decreasing permeability, making them suitable for reducing landslide incidences. The results of this study could be improved by utilizing factors such as the Normalized Difference Road Landside Index (Zhao et al. 2018) and topographic ruggedness index. This will be considered in future research.

Conclusions

Due to the geomorphological setting of the area, the Western Ghats region in Kollam district is prone to landslides. This study assessed the spatial relationship between the conditioning factors and landslide incidences using GIS. The AHP and FR models were used to identify the susceptibility. The area of the landslide susceptible zone maps was divided into different zones using the natural breaks method. The critical zones together constitute 33.3% (AHP

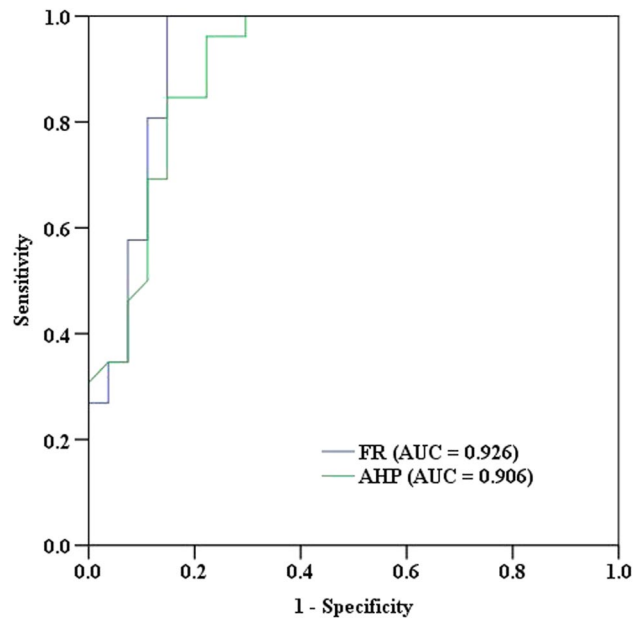


Fig. 16 The ROC curves

Table 6 Area and percentage of susceptible zones – AHP and FR method

Landslide susceptible zones	AHP method		FR method	
	Area (Sq. km)	Percentage of the area of the landslide susceptible zones	Area (Sq. km)	Percentage of the area of the landslide susceptible zones
Very low	125.83	16.23	163.15	21.04
Low	190.61	24.59	248.07	32.00
Moderate	200.60	25.88	181.14	23.37
High	169.16	21.82	124.76	16.10
Very high	88.98	11.48	58.06	7.49
Total	775.18	100	775.18	100

method) and 23.59% (FR method) of the study area. It was found that slope angle, elevation, streams, soil, and road cuttings are the major inducing factors. From the study, it is found that landslides prevailing in this region are due to natural as well as human-induced reasons. Finally, the prepared map was validated using the incidence data provided by NRSC. The ROC curve analysis proved that the FR method has better prediction accuracy than the AHP method for landslide-susceptible zone mapping. The rainfall (triggering factor) is not considered in this study due to the non-availability of an adequate network of rain gauges or automatic weather stations, and also because the available satellite-derived data and India Meteorological Department gridded data have very low spatial resolution, which will not yield good data for a smaller region like this. The developed framework and created maps are essential to the land use planners, researchers, and the local government for taking proper landslide preventive and mitigation measures in the study area. This will help to reduce the impacts of landslide disasters in the future.

Acknowledgements Authors would like to thank the National Remote Sensing Centre (NRSC), Hyderabad, India for providing landslide incidence data. Authors are thankful to Dr. Paolo Tarolli, Associate Professor, Department of Land, Environment, Agriculture and Forestry, University of Padova, Italy for the constructive comments which helped to improve the quality of the manuscript.

Data availability The datasets generated during and/or analyzed during the current study are available from the corresponding author on reasonable request.

Declarations

Conflict of interest The authors have no conflicts of interest to declare.

Ethical approval This article does not contain any studies with human participants or animals performed by any of the authors.

Informed consent Not applicable.

References

- Abrams W, Ghoneim E, Shew R, LaMaskin T, Al-Bloushi K, Hussein S, AbuBakr M, Al-Mulla E, Al-Awar M, El-Baz F (2018) Delineation of groundwater potential (GWP) in the northern United Arab Emirates and Oman using geospatial technologies in conjunction with Simple Additive Weight (SAW), Analytical Hierarchy Process (AHP), and Probabilistic Frequency Ratio (PFR) techniques. *J Arid Environ* 157:77–96. <https://doi.org/10.1016/j.jaridenv.2018.05.005>
- Achour Y, Boumezeur A, Hadji R, Chouabbi A, Cavaleiro V, Bendaoud EA (2017) Landslide susceptibility mapping using analytic hierarchy process and information value methods along a highway road section in Constantine, Algeria. *Arab J Geosci* 10. <https://doi.org/10.1007/s12517-017-2980-6>
- Achour Y, Pourghasemi HR (2020) How do machine learning techniques help in increasing accuracy of landslide susceptibility maps? *Geosci Front* 11(3):871–883. <https://doi.org/10.1016/j.gsf.2019.10.001>
- Ajin RS, Loghini AM, Vinod PG, Jacob MK, Krishnamurthy RR (2016) Landslide susceptible zone mapping using ARS and GIS techniques in selected taluks of Kottayam district, Kerala, India. *Int J Appl Remote Sens GIS* 3(1):16–25
- Akgun A, Dag S, Bulut F (2008) Landslide susceptibility mapping for a landslide-prone area (Findikli, NE of Turkey) by likelihood-frequency ratio and weighted linear combination models. *Environ Geol* 54:1127–1143. <https://doi.org/10.1007/s00254-007-0882-8>
- Aleotti P, Chowdhury R (1999) Landslide hazard assessment: summary review and new perspectives. *Bull Eng Geol Environ* 58:21–44. <https://doi.org/10.1007/s100640050066>
- Anbalagan R (1992) Landslide hazard evaluation and zonation mapping in mountainous terrain. *Eng Geol* 32(4):269–277. [https://doi.org/10.1016/0013-7952\(92\)90053-2](https://doi.org/10.1016/0013-7952(92)90053-2)
- Arce-Mojica Td, Nehren U, Sudmeier-Rieux K, Miranda PJ, Anhuf D (2019) Nature-based solutions (NbS) for reducing the risk of shallow landslides: Where do we stand? *Int J Disaster Risk Reduct* 41. <https://doi.org/10.1016/j.ijdrr.2019.101293>
- Ballabio C, Sterlacchini S (2012) Support vector machines for landslide susceptibility mapping: The Staffora river basin case study, Italy. *Math Geosci* 44:47–70. <https://doi.org/10.1007/s11004-011-9379-9>
- Beullens J, Van de Velde D, Nyssen J (2014) Impact of slope aspect on hydrological rainfall and on the magnitude of rill erosion in Belgium and northern France. *Catena* 114:129–139. <https://doi.org/10.1016/j.catena.2013.10.016>
- Bui DT, Pradhan B, Lofman O, Revhaug I (2012) Landslide susceptibility assessment in Vietnam using support vector machines, decision tree, and Naïve Bayes models. *Math Probl Eng*. <https://doi.org/10.1155/2012/974638>

- Catani F, Lagomarsino D, Segoni S, Tofani V (2013) Landslide susceptibility estimation by random forests technique: sensitivity and scaling issues. *Nat Hazards Earth Syst Sci* 13:2815–2831. <https://doi.org/10.5194/nhess-13-2815-2013>
- Chausson A, Turner B, Seddon D, Chabaneix N, Girardin CAJ, Kapos V, Key I, Roe D, Smith A, Woroniecki S, Seddon N (2020) Mapping the effectiveness of Nature-based Solutions for climate change adaptation. *Glob Change Biol* 26:6134–6155. <https://doi.org/10.1111/gcb.15310>
- Chawla A, Chawla S, Pasupuleti S, Rao ACS, Sarkar K, Dwivedi R (2018) Landslide susceptibility mapping in Darjeeling Himalayas, India. *Adv Civil Eng*. <https://doi.org/10.1155/2018/6416492>
- Dahal BK, Dahal RK (2017) Landslide hazard map: tool for optimization of low-cost mitigation. *Geoenviron Disasters* 4(8). <https://doi.org/10.1186/s40677-017-0071-3>
- Dai F, Lee C, Li J, Xu ZW (2001) Assessment of landslide susceptibility on the natural terrain of Lantau Island, Hong Kong. *Environ Geol* 40:381–391. <https://doi.org/10.1007/s002540000163>
- Dahal RK, Hasegawa S, Nonomura A, Yamanaka M, Masuda T, Nishino K (2008) GIS-based weights-of-evidence modelling of rainfall-induced landslides in small catchments for landslide susceptibility mapping. *Environ Geol* 54(2):311–324. <https://doi.org/10.1007/s00254-007-0818-3>
- Devkota KC, Regmi AD, Pourghasemi HR, Yoshida K, Pradhan B, Ryu IC, Dhital MR, Althuwaynee OF (2013) Landslide susceptibility mapping using certainty factor, index of entropy and logistic regression models in GIS and their comparison at Mugling–Narayanghat road section in Nepal Himalaya. *Nat Hazards* 65:135–165. <https://doi.org/10.1007/s11069-012-0347-6>
- El Jazouli A, Barakat A, Khellouk R (2019) GIS-multicriteria evaluation using AHP for landslide susceptibility mapping in Oum Er Rbia high basin (Morocco). *Geoenviron Disasters* 6(3). <https://doi.org/10.1186/s40677-019-0119-7>
- Elmoulat M, Ait Brahim L (2018) Landslide susceptibility mapping using GIS and weights of evidence model in Tetouan-Ras-Mazari area (Northern Morocco). *Geomatics Nat Hazards Risk* 9(1):1306–1325. <https://doi.org/10.1080/19475705.2018.1505666>
- Fatemi Aghda SM, Bagheri V, Razifard M (2018) Landslide susceptibility mapping using fuzzy logic system and its influences on mainlines in Lashgarak region, Tehran, Iran. *Geotech Geol Eng* 36:915–937. <https://doi.org/10.1007/s10706-017-0365-y>
- García-Rodríguez MJ, Malpica JA, Benito B, Díaz M (2008) Susceptibility assessment of earthquake-triggered landslides in El Salvador using logistic regression. *Geomorphology* 95(3–4):172–191. <https://doi.org/10.1016/j.geomorph.2007.06.001>
- Getachew N, Meten M (2021) Weights of evidence modeling for landslide susceptibility mapping of Kabi-Gebro locality, Gundomeskel area, Central Ethiopia. *Geoenviron Disasters* 8. <https://doi.org/10.1186/s40677-021-00177-z>
- Gobinath R, Ganapathy GP, Akinwumi II (2015) Evaluating the use of lemon grass roots for the reinforcement of a landslide-affected soil from Nilgris district, Tamil Nadu, India. *J Mater Environ Sci* 6(10):2681–2687
- Grimnes S, Martinsen ØG (2015) Chap. 9 - Data and models. In: Grimnes S, Martinsen ØG (eds) *Bioimpedance and bioelectricity basics*, 3rd edn. Academic, Cambridge, pp 329–404. <https://doi.org/10.1016/B978-0-12-411470-8.00009-X>
- Guzzetti F, Carrara A, Cardinali M, Reichenbach P (1999) Landslide hazard evaluation: a review of current techniques and their application in a multi-scale study. *Cent Italy Geomorphol* 31(1–4):181–216. [https://doi.org/10.1016/S0169-555X\(99\)00078-1](https://doi.org/10.1016/S0169-555X(99)00078-1)
- Hanley JA, McNeil BJ (1982) The meaning and use of the area under a receiver operating characteristic (ROC) curve. *Radiology* 143:29–36
- Hemasinghe H, Rangali RSS, Deshapriya NL, Samarakoon L (2018) Landslide susceptibility mapping using logistic regression model (a case study in Badulla District, Sri Lanka). *Procedia Eng* 212:1046–1053. <https://doi.org/10.1016/j.proeng.2018.01.135>
- Hosmer DW, Lemeshow S (2000) *Applied logistic regression*, 2nd edn. Chapter 5, Wiley, New York, pp 160–164
- Jana SK, Sekac T, Pal DK (2019) Geo-spatial approach with frequency ratio method in landslide susceptibility mapping in the Busu River catchment, Papua New Guinea. *Spat Inform Res* 27:49–62. <https://doi.org/10.1007/s41324-018-0215-x>
- Kanungo DP, Arora MK, Sarkar S, Gupta RP (2006) A comparative study of conventional, ANN black box, fuzzy and combined neural and fuzzy weighting procedures for landslide susceptibility zonation in Darjeeling Himalayas. *Eng Geol* 85(3–4):347–366. <https://doi.org/10.1016/j.enggeo.2006.03.004>
- Kanungo DP, Arora MK, Sarkar S, Gupta RP (2009) Landslide susceptibility zonation (LSZ) mapping - a review. *Journal of South Asia Disaster Studies* 2(1):81–105
- Karsli F, Atasoy M, Yalcin A, Reis S, Demir O, Gokceoglu C (2009) Effects of land-use changes on landslides in a landslide-prone area (Ardesen, Rize, NE Turkey). *Environ Monit Assess* 156. <https://doi.org/10.1007/s10661-008-0481-5>
- Lai C, Chen X, Wang Z, Xu CY, Yang B (2018) Rainfall-induced landslide susceptibility assessment using random forest weight at basin scale. *Hydrol Res* 49(5):1363–1378. <https://doi.org/10.2166/nh.2017.044>
- Lee S (2007) Landslide susceptibility mapping using an artificial neural network in the Gangneung area, Korea. *Int J Remote Sens* 28(21):4763–4783. <https://doi.org/10.1080/01431160701264227>
- Lee S, Choi J, Min K (2004) Probabilistic landslide hazard mapping using GIS and remote sensing data at Boun, Korea. *Int J Remote Sens* 25(11):2037–2052. <https://doi.org/10.1080/01431160310001618734>
- Lee S, Hong SM, Jung HS (2017) A support vector machine for landslide susceptibility mapping in Gangwon Province. *Korea Sustain* 9(1). <https://doi.org/10.3390/su9010048>
- Lee S, Lee MJ, Jung HS, Lee S (2019) Landslide susceptibility mapping using Naïve Bayes and Bayesian network models in Umyeonsan, Korea. *Geocarto Int*. <https://doi.org/10.1080/10106049.2019.1585482>
- Lombardo L, Mai PM (2018) Presenting logistic regression-based landslide susceptibility results. *Eng Geol* 244:14–24. <https://doi.org/10.1016/j.enggeo.2018.07.019>
- Mandal S, Maiti R (2014) Role of lithological composition and lineaments in landsliding: A case study of Shivkhola watershed, Darjeeling Himalaya. *Int J Geol Earth Environ Sci* 4(1):126–132
- Mohajane M, Essahlaoui A, Oudija F, Hafyani ME, Hmaid AE, Ouali AE, Randazzo G, Teodoro AC (2018) Land use/land cover (LULC) using Landsat data series (MSS, TM, ETM + and OLI) in Azrou Forest, in the Central Middle Atlas of Morocco. *Environments* 5(12). <https://doi.org/10.3390/environments5120131>
- Mohammed A, Wennian X, Zhenyao X (2018) Ecological and bioengineering studies for stabilizing the Wad Medani-Sennar roadside slope linking the Gezira and Sennar States. *Adv Civil Eng*. <https://doi.org/10.1155/2018/7430809>
- NDMA (2009) Management of landslides and snow avalanches. National Disaster Management Authority (NDMA), Government of India, New Delhi, p 144
- Nefeslioglu HA, Sezer E, Gokceoglu C, Bozkir AS, Duman TY (2010) Assessment of landslide susceptibility by decision trees in the metropolitan area of Istanbul, Turkey. *Math Probl Eng*. <https://doi.org/10.1155/2010/901095>
- Nguyen TTN, Liu CC (2019) A new approach using AHP to generate landslide susceptibility maps in the Chen-Yu-Lan Watershed, Taiwan. *Sensors* 19(3). <https://doi.org/10.3390/s19030505>
- Nikhil S, Danumah JH, Saha S, Prasad MK, Rajaneesh A, Mammen PC, Ajin RS, Kuriakose SL (2021) Application of GIS and AHP

- method in forest fire risk zone mapping: A study of the Parambikulam Tiger Reserve, Kerala, India. *J Geovisualization Spat Anal* 5. <https://doi.org/10.1007/s41651-021-00082-x>
- Oh HJ, Kadavi PR, Lee CW, Lee S (2018) Evaluation of landslide susceptibility mapping by evidential belief function, logistic regression and support vector machine models. *Geomatics Nat Hazards Risk* 9(1):1053–1070. <https://doi.org/10.1080/19475705.2018.1481147>
- Oh HJ, Lee S, Hong SM (2017) Landslide susceptibility assessment using frequency ratio technique with Iterative random sampling. *J Sens*. <https://doi.org/10.1155/2017/3730913>
- Ortiz JAV, Martínez-Graña AM (2018) A neural network model applied to landslide susceptibility analysis (Capitanejo, Colombia). *Geomatics Nat Hazards Risk* 9(1):1106–1128. <https://doi.org/10.1080/19475705.2018.1513083>
- Panchal S, Shrivastava AK (2021) Landslide hazard assessment using analytic hierarchy process (AHP): A case study of National Highway 5 in India. *Ain Shams Eng J*. <https://doi.org/10.1016/j.asej.2021.10.021>
- Pascale S, Parisi S, Mancini A, Schiattarella M, Conforti M, Sole A, Murgante B, Sdao F (2013) Landslide susceptibility mapping using artificial neural network in the urban area of Senise and San Costantino Albanese (Basilicata, Southern Italy). In: Murgante B, Misra S, Carlini M, Torre CM, Nguyen HQ, Taniar D, Apduhan BO, Gervasi O (eds) *Computational science and its applications – ICCSA 2013*, vol 7974. Springer, Berlin, Heidelberg, pp 473–488. https://doi.org/10.1007/978-3-642-39649-6_34
- Polykretis C, Chalkias C (2018) Comparison and evaluation of landslide susceptibility maps obtained from weight of evidence, logistic regression, and artificial neural network models. *Nat Hazards* 93:249–274. <https://doi.org/10.1007/s11069-018-3299-7>
- Pourghasemi HR, Jirandeh AG, Pradhan B, Xu C, Gokceoglu C (2013) Landslide susceptibility mapping using support vector machine and GIS at the Golestan Province, Iran. *J Earth Syst Sci* 122(2):349–369
- Pourghasemi HR, Mohammady M, Pradhan B (2012a) Landslide susceptibility mapping using index of entropy and conditional probability models in GIS: Safarod Basin, Iran. *Catena* 97:71–84. <https://doi.org/10.1016/j.catena.2012.05.005>
- Pourghasemi HR, Pradhan B, Gokceoglu C (2012b) Application of fuzzy logic and analytical hierarchy process (AHP) to landslide susceptibility mapping at Haraz watershed, Iran. *Nat Hazards* 63(2):965–996. <https://doi.org/10.1007/s11069-012-0217-2>
- Pradhan B, Oh HJ, Buchroithner M (2010a) Weights-of-evidence model applied to landslide susceptibility mapping in a tropical hilly area. *Geomatics Nat Hazards Risk* 1(3):199–223. <https://doi.org/10.1080/19475705.2010.498151>
- Pradhan B, Sezer EA, Gokceoglu C, Buchroithner MF (2010b) Landslide susceptibility mapping by neuro-fuzzy approach in a landslide-prone area (Cameron Highlands, Malaysia). *IEEE Trans Geosci Remote Sens* 48(12):4164–4177. <https://doi.org/10.1109/TGRS.2010.2050328>
- Prasannakumar V, Vijith H (2012) Evaluation and validation of landslide spatial susceptibility in the Western Ghats of Kerala, through GIS-based weights of evidence model and area under curve technique. *J Geol Soc India* 80(4):515–523. <https://doi.org/10.1007/s12594-012-0171-3>
- Quinn PE, Hutchinson DJ, Diederichs MS, Rowe RK (2010) Regional-scale landslide susceptibility mapping using the weights of evidence method: an example applied to linear infrastructure. *Can Geotech J* 47(8):905–927. <https://doi.org/10.1139/T09-144>
- Rahardjo H, Satyanaga A, Leong EC, Santoso VA, Ng YS (2014) Performance of an instrumented slope covered with shrubs and deep-rooted grass. *Soils Found* 54(3):417–425. <https://doi.org/10.1016/j.sandf.2014.04.010>
- Reguero BG, Beck MW, Bresch DN, Calil J, Meliane I (2018) Comparing the cost effectiveness of nature-based and coastal adaptation: A case study from the Gulf Coast of the United States. *PLoS ONE* 13(4). <https://doi.org/10.1371/journal.pone.0192132>
- Roslee R, Jamaluddin TA, Talip MA (2012) Landslide susceptibility mapping (LSM) at Kota Kinabalu, Sabah Malaysia using Factor Analysis Model (FAM). *J Adv Sci Eng Res* 2:80–103
- Rouse JW, Haas RH, Schell JA, Deering DW (1974) Monitoring vegetation systems in the Great Plains with ERTS. In: Freden SC, Mercanti EP, Becker M (eds) *Third Earth Resources Technology Satellite-1 Symposium*, vol I. Technical Presentations, NASA SP-351. NASA, Washington, D.C., pp 309–317
- Saaty TL (1980) *The analytic hierarchy process*. McGraw Hill, New York
- Saha AK, Gupta RP, Arora MK (2002) GIS-based Landslide Hazard Zonation in the Bhagirathi (Ganga) Valley, Himalayas. *Int J Remote Sens* 23(2):357–369. <https://doi.org/10.1080/01431160010014260>
- Saravanan S, Jegankumar R, Selvaraj A, Jennifer JJ, Parthasarathy KSS (2019) Chapter 20 - Utility of Landsat data for assessing mangrove degradation in Muthupet Lagoon, South India. In: Ramkumar M, James RA, Menier D, Kumaraswamy K (eds) *Coastal Zone Management*. Elsevier, pp 471–484. <https://doi.org/10.1016/B978-0-12-814350-6.00020-3>
- Sartohadi J, Pulungan NAHJ, Nurudin M, Wahyudi W (2018) The ecological perspective of landslides at soils with high clay content in the Middle Bogowonto watershed, Central Java, Indonesia. *Appl Environ Soil Sci*. <https://doi.org/10.1155/2018/2648185>
- Semlali I, Ouadif L, Bahi L (2019) Landslide susceptibility mapping using the analytical hierarchy process and GIS. *Curr Sci* 116(5):773–779. <https://doi.org/10.18520/cs/v116/i5/773-779>
- Setiawan I, Mahmud AR, Mansor S, Shariff ARM, Nuruddin AA (2004) GIS-grid-based and multi-criteria analysis for identifying and mapping peat swamp forest fire hazard in Pahang M. *Disaster Prev Manag* 13(5):379–386
- Shahri AA, Spross J, Johansson F, Larsson S (2019) Landslide susceptibility hazard map in southwest Sweden using artificial neural network. *Catena* 183. <https://doi.org/10.1016/j.catena.2019.104225>
- Shao X, Ma S, Xu C, Shen L, Lu Y (2020) Inventory, distribution and geometric characteristics of landslides in Baoshan City, Yunnan Province, China. *Sustainability* 12(6). <https://doi.org/10.3390/su12062433>
- Sharma LP, Patel N, Ghose MK, Debnath P (2012) Influence of Shannon's entropy on landslide-causing parameters for vulnerability study and zonation—a case study in Sikkim, India. *Arab J Geosci* 5:421–431. <https://doi.org/10.1007/s12517-010-0205-3>
- Sharma LP, Patel N, Ghose MK, Debnath P (2013) Synergistic application of fuzzy logic and geo-informatics for landslide vulnerability zonation—a case study in Sikkim Himalayas, India. *Appl Geomatics* 5:271–284. <https://doi.org/10.1007/s12518-013-0115-7>
- Sharma LP, Patel N, Ghose MK, Debnath P (2014) Application of frequency ratio and likelihood ratio model for geo-spatial modeling of landslide hazard vulnerability assessment and zonation: a case study from the Sikkim Himalayas in India. *Geocarto Int* 29(2):128–146. <https://doi.org/10.1080/10106049.2012.748830>
- Sharma LP, Patel N, Ghose MK, Debnath P (2015) Development and application of Shannon's entropy integrated information value model for landslide susceptibility assessment and zonation in Sikkim Himalayas in India. *Nat Hazards* 75:1555–1576. <https://doi.org/10.1007/s11069-014-1378-y>
- Sidle RC (2007) Using weather and climate information for landslide prevention and mitigation. In: Sivakumar MVK, Ndiang'ui N (eds) *Climate and land degradation*. Environmental Science and Engineering (Environmental Science) book series (ESE).

- Springer, Berlin, Heidelberg, pp 285–307. https://doi.org/10.1007/978-3-540-72438-4_15
- Silalahi FES, Pamela, Arifianti Y, Hidayat F (2019) Landslide susceptibility assessment using frequency ratio model in Bogor, West Java, Indonesia. *Geosci Lett* 6(10). <https://doi.org/10.1186/s40562-019-0140-4>
- Singh A, Sarma AK, Hack J (2020) Cost-effective optimization of nature-based solutions for reducing urban floods considering limited space availability. *Environ Processes* 7:297–319. <https://doi.org/10.1007/s40710-019-00420-8>
- Sujatha ER, Sridhar V (2021) Landslide susceptibility analysis: A logistic regression model case study in Coonoor, India. *Hydrology* 8(1). <https://doi.org/10.3390/hydrology8010041>
- Sur U, Singh P, Meena SR (2020) Landslide susceptibility assessment in a lesser Himalayan road corridor (India) applying fuzzy AHP technique and earth-observation data. *Geomatics Nat Hazards Risk* 11(1):2176–2209. <https://doi.org/10.1080/19475705.2020.1836038>
- Taalab K, Cheng T, Zhang Y (2018) Mapping landslide susceptibility and types using Random Forest. *Big Earth Data* 2(2):159–178. <https://doi.org/10.1080/20964471.2018.1472392>
- Thomas AV, Saha S, Danumah JH, Raveendran S, Prasad MK, Ajin RS, Kuriakose SL (2021) Landslide susceptibility zonation of Idukki district using GIS in the aftermath of 2018 Kerala floods and landslides: A comparison of AHP and frequency ratio methods. *J Geovisualization Spat Anal* 5. <https://doi.org/10.1007/s41651-021-00090-x>
- Tien PV, Luong LH, Nhat LM, Thanh NK, Cuong PV (2021) Landslides along Halong-Vandon expressway in Quang Ninh province, Vietnam. In: Guzzetti F, Arbanas SM, Reichenbach P, Sassa K, Bobrowsky PT, Takara K (eds) *Understanding and reducing landslide disaster risk, Volume2 - From mapping to hazard and risk zonation*. Springer Nature, Cham, pp 133–139. <https://doi.org/10.1007/978-3-030-60227-7>
- Trianawati N, Rahmafritria F (2016) The mapping of landslide proneness in mountain-based tourist destinations: An overview of remote sensing and geographic information system (GIS) method. In: Radzi SM, Hanafiah MHM, Sumarjan N, Mohi Z, Sukyadi D, Suryadi K, Purnawarman P (eds) *Heritage, Culture and Society: Research agenda and best practices in the hospitality and tourism industry*. CRC Press, Boca Raton, pp 473–476
- Turrini MC, Visintainer P (1998) Proposal of a method to define areas of landslide hazard and application to an area of the Dolomites, Italy. *Eng Geol* 50(3–4):255–265. [https://doi.org/10.1016/S0013-7952\(98\)00022-2](https://doi.org/10.1016/S0013-7952(98)00022-2)
- van Westen CJ, Castellanos E, Kuriakose SL (2008) Spatial data for landslide susceptibility, hazard, and vulnerability assessment: An overview. *Eng Geol* 102(3–4):112–131. <https://doi.org/10.1016/j.enggeo.2008.03.010>
- van Westen CJ, Jaiswal P, Ghosh S, Martha TR, Kuriakose SL (2012) Landslide inventory, hazard and risk assessment in India. In: Pradhan B, Buchroithner M (eds) *Terrigenous Mass Movements*. Springer, Berlin, Heidelberg, pp 239–282. https://doi.org/10.1007/978-3-642-25495-6_9
- Viana CM, Oliveira S, Oliveira SC, Rocha J (2019) 29 - Land use/land cover change detection and urban sprawl analysis. In: Pourghasemi HR, Gokceoglu C (eds) *Spatial Modeling in GIS and R for Earth and Environmental Sciences*. Elsevier, pp 621–651. <https://doi.org/10.1016/B978-0-12-815226-3.00029-6>
- Xu C, Dai F, Xu X, Lee YH (2012) GIS-based support vector machine modeling of earthquake-triggered landslide susceptibility in the Jianjiang River watershed, China. *Geomorphology* 145–146:70–80. <https://doi.org/10.1016/j.geomorph.2011.12.040>
- Yalcin A (2008) GIS-based landslide susceptibility mapping using analytical hierarchy process and bivariate statistics in Ardesen (Turkey): Comparisons of results and confirmations. *Catena* 72:1–12. <https://doi.org/10.1016/j.catena.2007.01.003>
- Yang H, Wang F, Vilfemek V, Araiba K, Asano S (2015) Investigation of rainfall-induced shallow landslides on the northeastern rim of Aso caldera, Japan, in July 2012. *Geoenviron Disasters* 2. <https://doi.org/10.1186/s40677-015-0028-3>
- Yilmaz I (2009) Landslide susceptibility mapping using frequency ratio, logistic regression, artificial neural networks and their comparison: A case study from Kat landslides (Tokat-Turkey). *Comput Geosci* 35(6):1125–1138. <https://doi.org/10.1016/j.cageo.2008.08.007>
- Youssef AM, Pourghasemi HR, Pourtaghi ZS, Al-Katheeri MM (2016) Landslide susceptibility mapping using random forest, boosted regression tree, classification and regression tree, and general linear models and comparison of their performance at Wadi Tayyah Basin, Asir Region, Saudi Arabia. *Landslides* 13:839–856. <https://doi.org/10.1007/s10346-015-0614-1>
- Zhang K, Wu X, Niu R, Yang K, Zhao L (2017) The assessment of landslide susceptibility mapping using random forest and decision tree methods in the Three Gorges Reservoir area, China. *Environ Earth Sci* 76. <https://doi.org/10.1007/s12665-017-6731-5>
- Zhao Y, Huang Y, Liu H, Wei Y, Lin Q, Lu Y (2018) Use of the normalized difference road landside index (NDRLI)-based method for the quick delineation of road-induced landslides. *Sci Rep* 8. <https://doi.org/10.1038/s41598-018-36202-9>

Publisher's Note Springer Nature remains neutral with regard to jurisdictional claims in published maps and institutional affiliations.